Heliyon 10 (2024) e32436

Contents lists available at ScienceDirect

Heliyon

journal homepage: www.cell.com/heliyon

Review article

Cardiac computed tomography with late contrast enhancement: A review

Davide Tore [a], Riccardo Faletti [a], Anna Palmisano [b], Sara Salto [a], Katia Rocco [a], Ambra Santonocito [a], Clara Gaetani [a], Andrea Biondo [a], Elena Bozzo [a], Fabio Giorgino [a], Ilenia Landolfi [a], Francesca Menchini [a], Antonio Esposito [b], Paolo Fonio [a], Marco Gatti [a,*]

[a] Radiology Unit, Department of Surgical Sciences, AOU Città Della Salute e Della Scienza di Torino, University of Turin, Turin, Italy
[b] Clinical and Experimental Radiology Unit, Experimental Imaging Center, IRCCS San Raffaele Scientific Institute, Milan, Italy

ARTICLE INFO

Keywords:
Late contrast enhancement
LCE
Cardiac CT
CCT
CMR
LGE
Tissue characterization

ABSTRACT

Cardiac computed tomography (CCT) has assumed an increasingly significant role in the evaluation of coronary artery disease (CAD) during the past few decades, whereas cardiovascular magnetic resonance (CMR) remains the gold standard for myocardial tissue characterization. The discovery of late myocardial enhancement following intravenous contrast administration dates back to the 1970s with ex-vivo CT animal investigations; nevertheless, the clinical application of this phenomenon for cardiac tissue characterization became prevalent for CMR imaging far earlier than for CCT imaging.

Recently the technical advances in CT scanners have made it possible to take advantage of late contrast enhancement (LCE) for tissue characterization in CCT exams. Moreover, the introduction of extracellular volume calculation (ECV) on cardiac CT images combined with the possibility of evaluating cardiac function in the same exam is making CCT imaging a multiparametric technique more and more similar to CMR.

The aim of our review is to provide a comprehensive overview on the role of CCT with LCE in the evaluation of a wide range of cardiac conditions.

1. Introduction

During the last decade, CCT has gained an increasingly important role in assessing coronary artery disease (CAD), although cardiovascular magnetic resonance (CMR) remains the gold standard for myocardial tissue characterization thanks to quantitative T1 and T2 mapping and late gadolinium enhancement (LGE) imaging.

Recent advances in CT scanner technology have enabled the use of late contrast enhancement (LCE) for tissue characterization in cardiac CT scans. In addition, the incorporation of extracellular volume calculation (ECV) on CCT images, coupled with the ability to evaluate heart function during the same test, is transforming CCT imaging into a multiparametric exam that increasingly resembles CMR.

The aim of this work is to provide an overview on the role of CCT with LCE in the evaluation of a wide range of cardiac conditions.

* Corresponding author.
E-mail address: m.gatti@unito.it (M. Gatti).

https://doi.org/10.1016/j.heliyon.2024.e32436
Received 31 December 2022; Received in revised form 19 May 2024; Accepted 4 June 2024
Available online 4 June 2024

2. Historical notes

Noninvasive characterization of myocardial tissue to distinguish between patterns of ischemic and non-ischemic myocardial damage is widely applied for diagnostic and prognostic purposes, particularly in CMR with LGE [1].

Indeed, the awareness of a difference in contrast enhancement between infarcted and non-infarcted myocardial tissue comes from research works published in the late 1970s on ex-vivo CTs of canine hearts with acute myocardial infarction. In these observations, infarcted tissue showed higher attenuation than normal myocardium, and these areas of enhancement matched with an increase in the uptake of technetium pyrophosphate (which is an infarct-avid radionuclide) and with regional differences in the distribution of thallium 201 (a metabolic marker) [2,3].

As confirmation, these regions of enhancement corresponded to the area of histologically confirmed myocardial infarction. These findings have been reproduced in retrospective ECG-gated CT scans in 1980s [4].

In a similar way, the concept of persistent enhancement at CMR of canine hearts extirpated after some minutes from the administration of gadolinium-based contrast media was established too [5].

Shortly thereafter, this phenomenon of late enhancement was demonstrated in alive canine infarcted hearts by ECG-gated T1-weighted CMR with the additional evidence of a different regional distribution of gadolinium that could also distinguish between those myocardial infarcted regions followed by re-perfusion and those who were not re-perfused [6].

This demonstration was followed by animal studies with the induction of progressive ischemia, which showed the absence of late enhancement in the reversibly injured myocardium and the presence of late enhancement only in irreversibly injured tissue [7,8].

Similar reports were published in men in the late 1980s [9,10].

Thereafter, technical improvements in CMR along with the introduction of sequences which improved contrast between normal and infarcted myocardium, led to the widespread clinical application of LGE CMR imaging to demonstrate the presence, the transmural extent, and size of myocardial scars. Lately, the application of gadolinium based CMR was extended to other types of cardiomyopathies, while the presence and the extent of myocardial damage/fibrosis started to be recognized as a predictor of adverse events, like ventricular remodeling, arrhythmias, and sudden cardiac death [11].

Since CMR is limitedly available due to the long acquisition times and unfeasible in claustrophobic patients or in patients with implantable devices, technological improvement has progressively transformed also CCT into a technique able both to comprehensively assess the anatomy of the heart and to obtain the characterization of myocardial damage or scars by LCE. In fact, CCT spatial and temporal resolution progressively improved with contemporary reduction in radiation exposure [12] and iodine contrast media shares the same kinetics and dynamics of gadolinium-based contrast agents, with delayed wash-out in scarred myocardium compared to the normal one.

In the latest years different research demonstrated that myocardial tissue characterization by LCE CCT was comparable to the one obtained by CMR [13], with specific patterns for each cardiomyopathy, e.g., ischemic cardiomyopathy, hypertrophic cardiomyopathy (HCM), or sarcoidosis [14–16].

Table 1
Main events in development of late enhancement cardiac imaging.

		Notable works
Late 1970s	First ex-vivo CTs studies on canine hearts demonstrating different contrast enhancement between infarcted and non-infarcted myocardial tissue.	Siemers et al. Detection, Quantitation and Contrast Enhancement of Myocardial Infarction Utilizing Computerized Axial Tomography: Comparison With Histochemical Staining and 99mTc-Pyrophosphate Imaging. 1977[3].
1980s	Demonstration of the same results in retrospective ECG-gated CT scans on canine model.	Dohertyet al. Detection and Quantitation of Myocardial Infarction In Vivo Using Transmission Computed Tomography; 1981 [4]
Late 1980s	CMR demonstration of persistence of gadolinium-based contrast media on canine infarcted heart models. -Late enhancement demonstration in alive canine infarcted hearts on ECG-gated T1-weighted CMR. -Differentiation between re-perfused and non-re-perfused ischemic areas.	McNamara et al. Acute Myocardial Ischemia: Magnetic Resonance Contrast Enhancement with Gadolinium-DTPA1; 1984 [5] Tscholakoff et al. Occlusive and Reperfused Myocardial Infarcts: Effect of Gd-DTPA on ECG-Gated MR Imaging; 1986 [6]
	-Animal studies confirmation of late enhancement persistence in permanently injured myocardial tissue and absence of late enhancement in reversible damaged myocardium. -First studies on men reporting similar results.	Eichstaedt et al. Magnetic Resonance Imaging (MRI) in Different Stages of Myocardial Infarction Using the Contrast Agent Gadolinium-DTPA; 1986 [10]
1990s–2000s	-Technical improvements in CCT and first experiences in tissue characterization	Gerber et al. Characterization of Acute and Chronic Myocardial Infarcts by Multidetector Computed Tomography: Comparison with Contrast-Enhanced Magnetic Resonance; 2006 [13]
2010s	-Application of LGE in CMR in other cardiac diseases (e.g., cardiomyopathies). -LGE-CMR role as predictor of adverse events (e.g., ventricular remodeling, arrhythmias, sudden cardiac death).	Chan et al. Prognostic Value of Quantitative Contrast-Enhanced Cardiovascular Magnetic Resonance for the Evaluation of Sudden Death Risk in Patients with Hypertrophic Cardiomyopathy; 2014 [11]
2020 and later	-Myocardial tissue characterization by late contrast enhancement CCT comparable to LGE CMR imaging. -CCT as a cardiac multiparametric imaging modality -Introduction on market of Photon counting CT scanner	Palmisano et al. Myocardial Late Contrast Enhancement CT in Troponin-Positive Acute Chest Pain Syndrome; 2021 [17]

The main events in late enhancement cardiac imaging are resumed in Table 1.

3. Physiologic mechanism of late contrast enhancement

The rationale behind iodine LCE in CCT of compromised cardiac tissue relies on the same mechanisms of delayed gadolinium-enhancement in CMR, given the similar pharmacokinetics properties shared by these two classes of contrast media.

After bolus injection the contrast agent spreads from the intravascular compartment to the extracellular compartment, but its diffusion to the intracellular compartment is blocked in physiological tissue by the lipid cellular membrane [18,19].

An expanded local distribution volume of contrast medium can thus be seen in case of increase in the extravascular–extracellular space (in cardiomyopathies through the expansion of the interstitial space) or if cell membrane integrity is lost due to damage.

The differences in contrast agent distribution volumes are best appreciated a few minutes after injection, when equilibrium concentrations in the blood pool and in cardiac tissue have been reached. In case of ischemic lesions, the distribution volume of the contrast medium is not homogeneous, with lower contrast concentration at the periphery than at the core, demonstrating the peri-infarcted zone where non-viable cells are mixed with viable ones.

Moreover, myocardial enhancement depends on local perfusion, altered by microvascular obstruction in scarred tissue, as well as the intrinsic properties of the contrast agent.

Other pathologic conditions such as myocarditis, cardiomyopathies and infiltrative diseases can show a delayed enhancement due to the same mechanism [20].

Injured cardiac tissue can thus be discriminated on its different regional concentration of contrast medium on late acquisitions (10–15 min) [21].

4. Technical aspects

The LCE scan should be acquired 7–10 min after contrast injection. A full dose of contrast medium, as for a standard body exam, is recommended to obtain a sufficient differentiation between healthy and pathologic myocardium. The LCE images should be acquired with low kV parameters (e.g., 80 kV) with single source scanners to enhance differences in the concentration of iodine contrast between scarred and non-scarred myocardium.

Dual-energy or spectral CT may represent a better choice to improve image quality in LCE imaging using low voltage (keV) monoenergetic and iodine density reconstructed images.

A comprehensive LCE CCT protocol may include a non-contrast acquisition, a whole-cycle CCTA acquisition with multiphase reconstruction [22], and the LCE scan.

The whole-cycle multiphase acquisition permit to assess cardiac ejection fraction and to identify motion abnormalities of the left ventricle walls. Cine-CT images can be reformatted in short-axis and long-axis, in four-chamber and three-chamber views, as usually seen on Cine-CMR sequences. Wall motion abnormalities can thus be correlated with LCE CCT scans to further improve LCE sensitivity and specificity.

LCE CCT scans are usually evaluated by reformatting them in the short-axis view, with section thickness of around 8–10 mm with 0 gap, in average mode. A myocardium scar is defined as a focal area of increased attenuation compared to the surrounding myocardium [23]. The scar-pattern may be non-ischemic or ischemic, it can be evaluated in its transmural extension and segmental cardiac involvement similarly to LGE CMR.

Extracellular volume fraction (ECV), an important staple of CMR [24], can be calculated on CCT images with a subtraction-derived method by drawing regions of interest (ROIs) on left ventricular myocardium and blood pool, extracting their attenuation values before and after the injection of iodine contrast medium, and correcting it for hematocrit [25–27].

ECV values are considered increased when they are 27 % or higher [28–30]. ECV values diffusely higher than 45 % are suggestive for cardiac amyloidosis [30].

Scar contrast-to-noise ratio (CNR) is defined as the difference in attenuation values between hyperattenuating and normal myocardium, divided by the standard deviation (SD) of normal myocardium attenuation (as in, derived from a ROI of at least 10mm2) [14].

5. Post processing

5.1. ECV calculation

Many common pathological mechanisms affecting myocardium (such as inflammation or ischemia) have edema and myocardial fibrosis as common manifestations, either focal or diffuse [31].

Currently the gold standard non-invasive technique to investigate myocardial fibrosis, edema and accumulation of extracellular material is CMR with LGE, due to its high contrast and spatial resolution [32]. This technique showed good correlation with tissue characterization by anatomopathological sections [33].

Moreover, recently the quantification of myocardial ECV with CMR has become an accepted parameter to assess various cardiac diseases. ECV fraction represents the percentage of the extracellular space in the myocardium and it is strongly correlated with the histological measurements of the extracellular matrix. Therefore, it acts as an important diagnostic biomarker of ventricular cardiac disease, as well as a possible biomarker of disease progression [34].

Since the pharmacokinetic of iodine contrast materials is comparable to those of gadolinium-based contrast materials, both diffusing rapidly and passively from the vascular space into extracellular tissue but not into the intracellular space (namely extracellular, extravascular contrast agents), CCT emerged as a valuable alternative to CMR in the quantification of fibrosis through late iodine enhancement and in ECV calculation [27,35].

The calculation of ECV with CMR reflects the equilibrium of gadolinium contrast agent between the myocardium and the blood pool and it is derived from pre- and postcontrast enhanced T1 mapping acquisitions [36].

Both CMR and CCT use an intravenous contrast material bolus, which enters the myocardium with a concentration gradient ("wash-in phase") and in a given time period it is cleared and returns to the bloodstream with a reverse concentration gradient ("wash-out phase"). This happens rapidly in healthy myocardium, while in damaged myocardium (focal or diffuse fibrosis), this pharmacokinetic is delayed due to multiple vascular factors (as differences in coronary flow, capillary permeability, functional capillary density, cellular membrane damage) and to the presence of a dense collagen matrix. Since the scar has an increased volume of extracellular water compared to healthy myocardium, at a certain time after bolus injection, there will be more contrast agent in the scar than in the blood or remote myocardium and measurable signal of the scar will therefore be increased [37].

If in CMR, relaxation rates (R1 or 1/T1) are directly proportional to the concentration of gadolinium and ECV is calculated as below:

$$\mathrm{ECV_{CMR}} = (1 - \mathrm{hematocrit}) \times \frac{\Delta\left(1/\mathrm{T1_{myo}}\right)}{\Delta\left(1/\mathrm{T1_{blood}}\right)}$$

where Δ(1/T1) is the difference between pre- and post-contrast relaxation rates [i.e. (R1myo post-contrast – R1myo pre contrast)/(R1 blood post-contrast – R1blood pre contrast)] [30].

In the same way in CT attenuation values (graded as Hounsfield units, HU) are directly proportional to the concentration of iodine contrast agent and ECV is calculated as:

$$\mathrm{ECV_{CT}} = (1 - \mathrm{hematocrit}) \times \frac{\Delta\mathrm{HU_{myo}}}{\Delta\mathrm{HU_{blood}}}$$

where ΔHU is the difference in HU attenuation pre- and post-contrast (i.e., HUpost-contrast – HUpre-contrast) [27,30].

Myocardial ECV calculation by cardiac CT was first validated in human in 2012 [38].

Recent research has demonstrated that there are no significant differences in ECV values measured with CMR and CT, both in healthy subjects and subjects affected by amyloidosis, HCM, DCM, and sarcoidosis [39].

This calculation requires pre- and post-contrast imaging, which might be burdened by misregistration errors due to difficulties to differentiate between myocardium and blood pool on pre contrast sequences, particularly among patient with irregularities in heart rate. Nowadays this limitation could be overcome by dual energy CT, in which ECV measurements could be performed only on the iodine maps, without the need for pre-contrast scan [40,41].

Recently a more efficient way of calculating ECV where the hematocrit of blood is derived from the attenuation of the blood pool (as the relationship between hematocrit and HU is linear) has been implemented to overcome the need for hematocrit blood test, simplifying the ECV workflow and permitting to display instantly ECV maps [27].

5.2. Scar burden quantification

The burden of fibrotic myocardium due to the underlying disease (i.e., scar burden) could be estimated by CMR and cardiac CT as the ratio between damaged myocardium and the entire LV mass identified on late contrast enhancement images. The percentage of LIE could be obtained by manual segmentation using a dedicated software or through semi-automated and automated methods. These approaches are currently under development or validation for the CMR field but soon could be extended to CT images, too [21,42].

In the end, new experimental selective contrast agents aimed at implementing scar detection are on trial, like AuNPs on gold nanoparticles functionalized with collagen-binding adhesion protein 35 (CNA35) which can achieve a prolonged blood pool enhancement for imaging coronary arteries and it can specifically target collagen within cardiac scars [43].

6. Clinical applications of late contrast enhancement

6.1. Ischemic heart disease

Ischemic heart disease is one of the most important causes of death and disability.

Myocardial infarction is a clinical condition characterized by insufficient blood provision to the cardiac tissue that ends with the myocardial cell death, and it is defined by a symptomatic acute myocardial damage associated with an important rise of troponins and, sometimes, EKG alterations [44].

The severity of myocardial infarction lies in its complications that can be mechanical, such as left ventricle aneurysm (LVA) and left ventricle pseudoaneurysm (LVP), or not mechanical [45].

LVA occurs days or weeks after a STEMI and commonly affects the anterior wall because of an occlusion of the left anterior descending artery [46].

Over time the aneurysmal wall becomes fibrotic and fragile because of the continuous high pressure inside the ventricle that stretches the infarcted myocardial zone which becomes larger and thinner [46].

This situation can easily end in the rupture of the ventricle wall, or it can generate an organized hematoma or a thrombus, due to the blood that remains confined inside the aneurysm.

False aneurysms, or LVP, it is a rupture of the free wall of left ventricle contained by epicardium, pericardial adhesions, or both. Usually, it occurs on the posterior and lateral ventricle wall. It uses to have a smaller neck compared to the aneurysm and a higher propensity to rupture, this is the reason why it is necessary a fast diagnosis and management [46,47].

Frequently LVP is an incidental diagnosis during routine imaging, or it is discovered in post-mortem, because usually is asymptomatic [48].

False aneurysm is very rare (less than 0.5 %) but potentially lethal, because its spontaneous evolution is related to false cavity rupture with sudden death by tamponade [45–48]. Rarely it can lead in a progressive enlargement of the pseudo aneurysmal cavity that could provoke heart failure signs such as ventricular arrhythmias or may evolve in thromboembolic complications [46].

Urgent surgery is the treatment of choice for LVP larger than 3 cm in diameter, symptomatic ones and for those discovered less than 3 months after infarction episode [45].

The correct diagnosis of MI complications is fundamental to evaluate patients' clinical conditions and subsequent management.

Chronic myocardial infarction is characterized by specifics ventricle wall changes, such as abnormalities in ventricle perfusion and contractions, changes in myocardial wall characteristics like fatty metaplasia or ventricle remodeling [49].

Generally transmural necrosis is its typical ischemic pattern, even if it could also be subendocardial; the quantity of the wall affection usually depends on the amount of time that myocardial cells remain without blood supply.

The pattern of LCE in ischemic heart disease is ischemic with wall involvement from subendocardial to transmural, an example of ischemic LCE pattern is reported in Fig. 1.

CCT scan can identify the exact region of the ventricle wall affected by the infarction by studying the heart kinetic with Cine-CT imagines [22]. In fact, it is possible to detect which region does not contract properly and it is also possible to study the myocardial perfusion by using iodine maps that show contrast distribution in the heart walls [40].

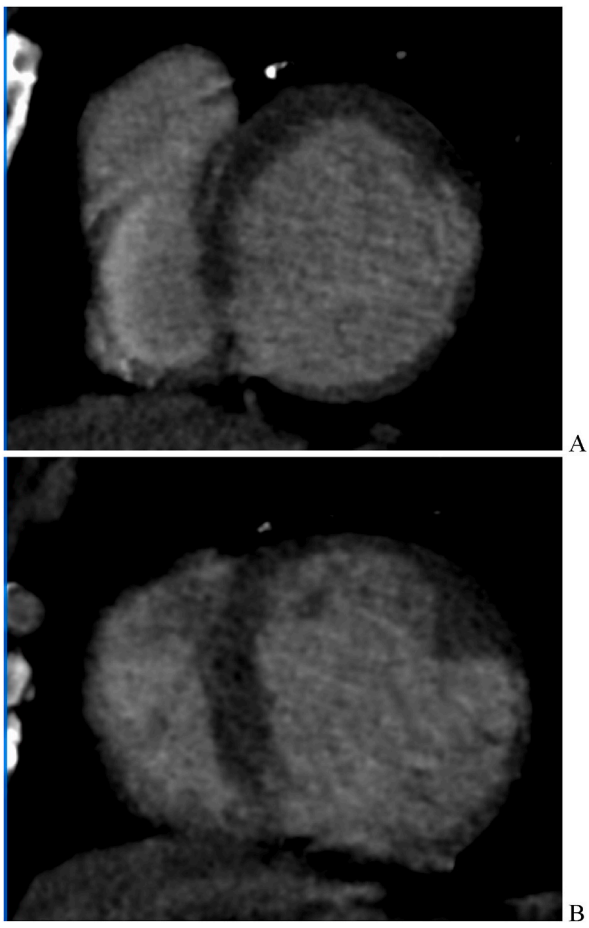

Fig. 1. Panel A and B. patient with ischemic heart disease, the myocardium is thinned in infero-septal, inferior and inferolateral ventricle wall with subendocardial LCE.

These maps are created by using images of all the three planes and thanks to a color code it can be easy to visually detect an alteration in wall perfusion. Generally grey corresponds to the normal wall and orange for a high contrast presence. An abnormal perfusion can be detected by seeing an altered color that usually affected the whole wall thickness (transmural), surrounded by normal myocardium [40].

Another instrument to evaluate the myocardial scar it is a map of grey's shades, thanks to a dual-energy CT scan, in which one tube it is generally set at 140 kV and the other at 100 kV, and it is possible to reconstruct images in this kV spectra. This it is useful because some materials have different characteristics within the CT spectrum used and it can be used to demonstrate the differences in Hounsfield Unit between the normal myocardium and the affected one [49].

Another important tool is the possibility of measuring the ECV (extracellular myocardium volume) using both phases pre and postcontrast to study the distributions of contrast in the myocardial wall. This is useful to differentiate several wall's pathologies; for example, patterns like myocarditis uses to have a higher ECV percentage (over 30 %) or myocardial scars that usually have a lower percentage (less than 25 %) [30,50].

The CCT scan protocol for comprehensive evaluation of patient with ischemic heart disease should include a non-contrast acquisition, that may show the presence of calcium in coronary arteries, in the valves, or in other parts, followed by contrast enhanced acquisition that allows the evaluation of coronary arteries and also myocardial perfusion. It is very useful to conclude the exams with a late contrast enhancement phase because it permits to recognize myocardial scars, wall necrosis and their extension [22].

It is possible to differentiate normal myocardial wall from the affected area, due to the presence of fibrosis in the scar. The contrast washout is slower if there is fibrosis and there is still enhancement about 8–10 min after the contrast injection; while normal myocardium at that time it's already cleared [2,4,40,51,52].

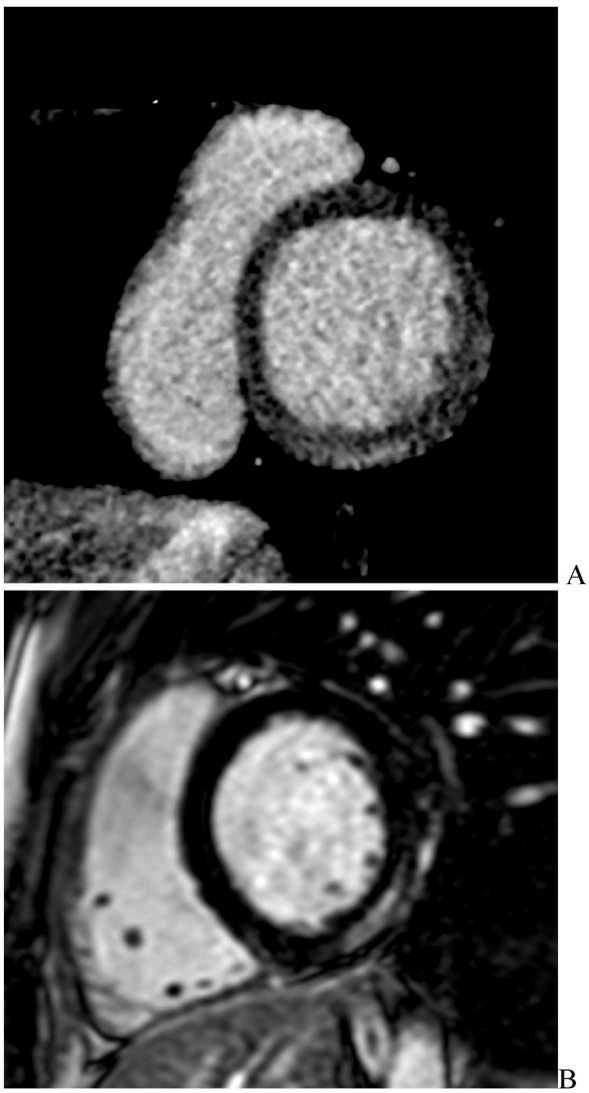

Fig. 2. Patient with myocarditis. Panel A subepicardial infero-lateral midwall LCE. In panel B LGE on CMR in the same location.

LCE phase could also be useful in patient without a clear episode of angina and with a normal early phase of coronary - CT-scan, as LCE imaging allows differential diagnosis of several other cardiac conditions such as myocarditis or infarction with unobstructed coronary arteries (MINOCA) [22].

CCT it is a very important also to identify MI complication such as differentiate a true aneurysm from a pseudoaneurysm. This is essential for the patients management because LVP has a higher susceptibility for rupture [45].

Using CT scan for patients' follow-up it is possible to evaluate how LVA and LVP are developing and the myocardial wall changes. Thanks to an early scan imaging, it is possible to verify if LVA and LVP dimensions are increasing and if there are thrombus inside the ventricle or not, and the variations of the cardiac contraction through the time [46,48].

While, thanks to the late contrast enhancement phase, it is possible to evaluate the changes of the amount of fibrosis.

Examination of patients in stable conditions can be done with both CT and MRI because as been demonstrated that there is a good agreement in the LCE findings and about the ECV percentage.

In case of emergency CCT scan may be preferable because the urgency of the situation leads to choose the fastest method of evaluation.

6.2. Non ischemic heart disease

6.2.1. Myocarditis

Diagnosis of myocarditis may be challenging due to the variety of clinical presentations and to the wide heterogeneity of underlying causes that have been described (viral, immune, inflammatory, …). Presenting symptoms may spread from minor settings of chest pain and palpitations along with temporary ECG changes up to life-threatening conditions such as cardiogenic shock or ventricular arrhythmias. Individuals of all ages may be affected by this pathological condition, although it is most frequent in the young. Even if histological, immunological and immunohistochemical criteria are the most reliable however endomyocardial biopsy (EMB) is becoming less and less common [53].

In clinical practice, non-invasive techniques such as CCT angiography (CCTA) and CMR are used respectively to rule out obstructive CAD and to confirm the suspect of myocarditis and monitor the disease progression. CMR is generally performed in clinically stable patients prior to EMB, as reported in literature, providing excellent tissue characterization, and supporting the diagnosis of myocarditis according to the modified-Lake Louise Criteria [54].

The LCE pattern of myocarditis is the same as in CMR: non ischemic, patchy, with general involvement of inferior-lateral ventricle wall. An example of patient with myocarditis is reported in Fig. 2.

Continuous improvements in CT technology are leading to further clinical application of CCT: dual-energy technology demonstrates promising results in the improvement of contrast-to-noise ratios for pathologic lesions in low-kilovolt-peak tube settings, along with the depiction and analysis of iodine accumulation in different tissues [54].

In case of suspected myocarditis, it is compulsory to exclude obstructive CAD and other causes of acute chest pain that could explain the clinical presentation, especially in patients with troponin-positive acute chest pain. On this side CCTA imaging performed in a recently proposed multiparametric "one-stop shop" protocol permits the simultaneous evaluation of coronary artery anatomy, pulmonary embolism, myocardial inflammation, to evaluate the presence and pattern of myocardial scar, ECV measurement with its relative degree and pattern of alteration [21,55].

Moreover, CCTA can always counts on its economic convenience and distribution making this technique suitable for the emergency setting as well as for the follow up., especially and to evaluate patients with contraindication to CMR (for example subjects with MR-unsafe implanted devices, claustrophobia, low compliance) significantly shortening the examination time [56].

6.2.2. Takotsubo cardiomyopathy

Takotsubo cardiomyopathy (TC) is a complex syndrome, with unclear pathophysiology, commonly related to emotional stresses as trigger event which leads to transient heart failure with myocardial injury/reversable stunning recently categorized as myocardial infarction with non-obstructive coronary arteries (MINOCA) [57].

The syndrome commonly presents with chest pain with or without dyspnea, especially in post-menopausal women, typically causing left ventricular apical ballooning, transient systolic dysfunction of the apex and mid-segments; the prognosis is generally favorable.

Diagnosis is often tricky: even if in TC regional wall motion abnormalities usually involve more than a single epicardial vascular territory, obstructive single-vessel coronary lesions are not an absolute criterion of exclusion, making the differential diagnosis from acute anterior STEMI sometimes extremely difficult [58,59].

In the diagnostic workflow of TC echocardiography plays an important role and CMR is obviously more accurate for qualitative and quantitative assessment of regional wall motion abnormalities, to quantify right and left ventricular volumes and function, tissue characterization and for the additional value of LGE sequences. However, because of the temporary nature of myocardial injury in TC LGE is usually absent, at least at high signal intensity thresholds [60].

The role of CCT has recently been particularly stressed thanks to the last technological developments: this non-invasive and more accessible and less time-consuming imaging technique permits the simultaneous evaluation of epicardial coronary arteries, to rule out CAD, pulmonary arteries and myocardial tissue characterization, representing a valid alternative to invasive angiography especially in hemodynamically stable patients with no ST-elevation at onset and clinical and echocardiography findings consistent with TC. CCT may also be preferred in patients with possible TC recurrence or in other critical clinical conditions associated with TC (i.e., stroke, sepsis, subarachnoid hemorrhage).

CCT definitively is a good choice for a comprehensive evaluation of patients with acute chest pain, doubtful TC, to rule out life-threatening conditions, with the additional value of late iodine enhancement acquisition. The importance of LCE imaging has been demonstrated observing a positive correlation between diffuse LCE in the mid and apical portion of the LV and the persistence of motion abnormalities after 1 month [61].

A volume rendering of the left ventricle cavity demonstrating akinesia and ballooning of the basal segments in a patient with reverse TC syndrome is reported in Fig. 3.

6.2.3. *Dilated cardiomyopathy*

Idiopathic dilated cardiomyopathy (IDCM) is defined as left ventricular (LV) dilatation associated with systolic dysfunction (LV ejection fraction less than 55 %) without signs of hypertensive disease, valvular heart disease or obstructive coronary artery disease. It represents the most common non-ischemic cardiomyopathy and the terminal form of multiple non-ischemic cardiomyopathies.

The use of CMR with the LGE technique represents the best way to assess myocardial fibrosis, often detected in dilated cardiomyopathy and associated with reduced systolic and diastolic function of the ventricle. Three types of delayed enhancement can be identified with LGE-CMR: midwall, subendocardial, transmural.

Linear or bandlike midwall delayed enhancement has been observed in 30 % of patients with IDCM [51].

The presence of myocardial delayed enhancement has been demonstrated as a strong predictor of adverse events not only in late-stage patients, but also in asymptomatic or mildly symptomatic ones [62].

The role of CCT is crucial in the diagnosis of IDCM, as it allows a combined evaluation of the coronary arteries, to exclude obstructive CAD (due to its high negative predictive value) essential for the diagnosis of IDCM, and of the myocardium.

Esposito et al. demonstrated how some important myocardial texture features (LCE and ECV) can be extracted from CCT examinations, and these provide decisive information on myocardial microstructural modifications useful for discriminating heart disease and in particular between post-ischemic dilated cardiomyopathy (ICD) and idiopathic cardiomyopathy (IDCM) [63].

Otha et al. pointed out that measuring ECV with IDI (Iodine Density Image) could facilitate the assessment of small regional areas of myocardial fibrosis, differentiating ischemic and non-ischemic patterns [64]. If this measurement is combined with simultaneous evaluation of the coronary circulation, an earlier diagnosis and more effective treatment could be achieved.

Another study illustrated a difference in Iodine density and ECV between patients with NIDCM (non-ischaemic dilated cardiomyopathy) and the control group, allowing them to discriminate between myocardium with NIDCM and healthy myocardium. The

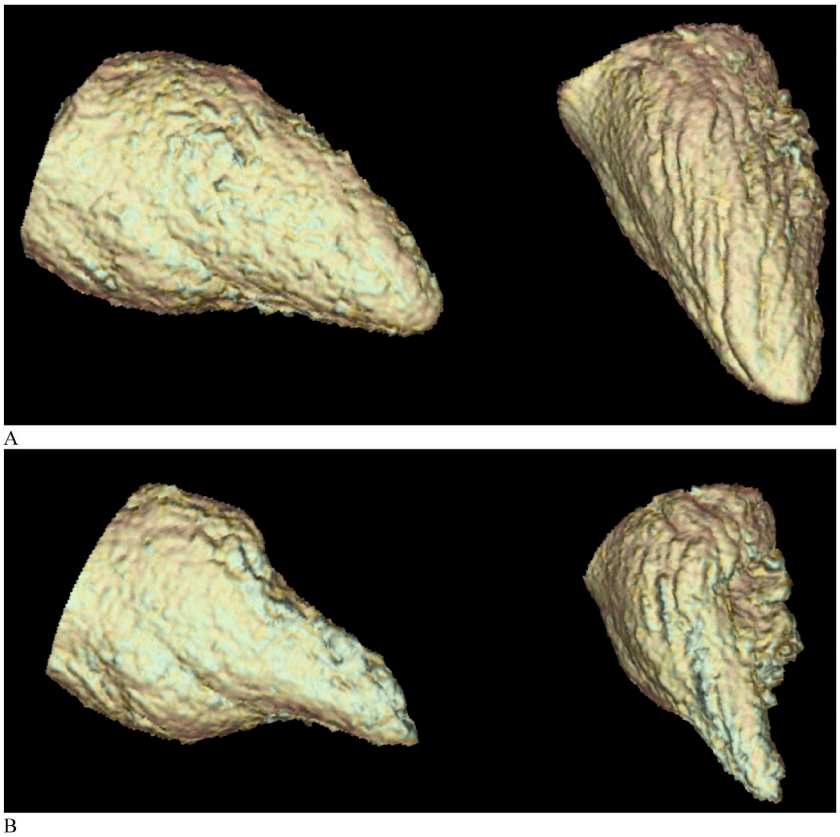

Fig. 3. Patient with reverse Takotsubo syndrome. Volume rendering of the left ventricle cavity demonstrating akinesia and ballooning of the basal segments (panel A diastole, panel B systole).

study also highlighted that the diagnostic performance was equal to or better than that of CMR, since CT measurements were performed for the whole myocardium while in some studies T1 mapping, to calve myocardial ECV, was performed on one or three slices (basal, mid and apical) [40,65].

As is well known, sudden cardiac death might be the first clinical manifestation of IDCM, but other arrhythmias may worsen the prognosis of patients. It has been observed that delayed enhancement affecting 25–75 % of the myocardial wall, especially in the basal or septal subvalvular site, represented a predictive factor for inducible ventricular tachycardia [66].

6.2.4. *Hypertrophic cardiomyopathy*

Hypertrophic cardiomyopathy (HCM) represents the most common primary cardiomyopathy, and it is characterized by diffuse or segmental hypertrophy of the LV, contributing to the development of intra-myocardial fibrosis. Frequently, the systolic function is preserved and there is an absence of compensatory dilatation of the cardiac chambers until the end stage, known as the burnout or dilated phase.

For the diagnosis of HCM, the maximum myocardial wall thickness must be precisely measured in diastolic phase: it is pathological if it exceeds 15 mm in end-diastole. However, since the most common form of HCM is asymmetrical septal hypertrophy, a ratio between the septum and inferolateral LV wall >1.3 (1.5 in hypertensive patients) is required for diagnosis [67].

Other well-known variants are the concentric, mid-ventricular, apical, or mass-like form.

The most feared complication is sudden cardiac death, and it has been reported in literature that an LV thickness >30 mm represents the cut-off for increased risk.

Currently, the gold standard for diagnosis is CMR, which allows evaluation of both ventricle volume and LGE, highlighting the presence of myocardial fibrosis.

In HCM, the distribution of LGE is usually patchy, located at the insertion sites of the right ventricle, and less frequently it is diffuse.

The presence of LGE, associated with an increase in ventricular muscle mass (LV-MM), is a highly important prognostic factor and is associated with the occurrence of adverse myocardial events [68].

The role of multidetector CCT in the diagnosis of HCM has been preliminarily linked to the evaluation of morphological signs of disease including the presence and localization of hypertrophy - with a slight overestimation of mean myocardial thickness compared to CMR [16], presence of crypts and evaluation of systolic function. Recently, its use has been increasingly gaining importance in the study of myocardial fibrosis.

Several studies have shown that the results obtained by CCT for the assessment of LCE and ECV can have a diagnostic accuracy superimposed on that of CMR [16,69,70]. In particular it has been observed that the prevalence of LCE is 58 % well correlated with histologic data, supported by a recent meta-analysis on CMR reporting a pooled prevalence of LGE of approximately 60 % [68].

These results, coupled with the possibility of simultaneously assessing the coronary arteries to exclude signs of CAD, underline the important role of CCT in the diagnosis of HCM, particularly in patients with contraindications to undergo CMR. An example of patient with HCM and LCE is reported in Fig. 4.

The analysis of ECV calculated with LCE CCT showed that mean ECV values in patients with HCM are significantly higher compared to healthy subjects.

6.2.5. *Sarcoidosis*

A frequent cause of restrictive cardiomyopathy is sarcoidosis (see Fig. 5). This granulomatous multisystemic disease, which has an unknown etiology, affects the heart in 5–10 % of patients and it is the second-most prevalent clinical presentation after lung disease [71].

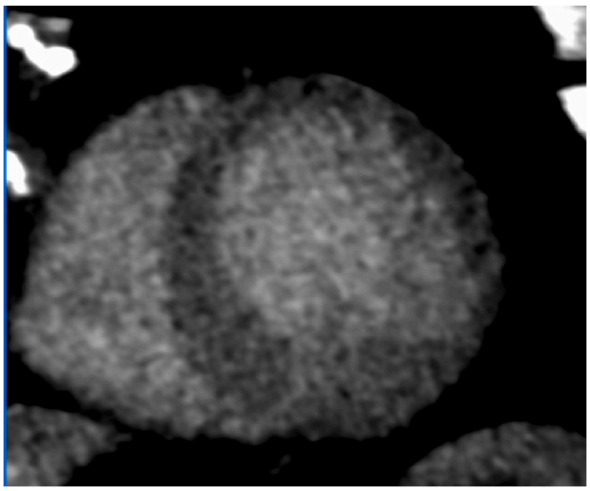

Fig. 4. Patient with HCM. Hypertrophy of the apical segments with LCE in the inferolateral wall.

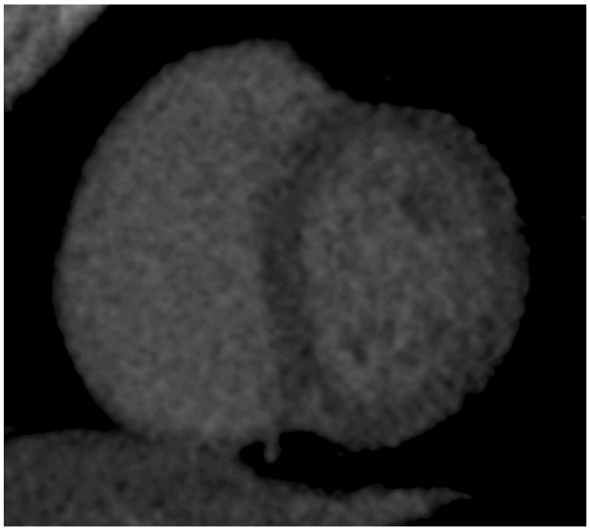

Fig. 5. Patient with history of sarcoidosis. LCE with non-ischemic pattern at the inferior hinge point.

Cardiac sarcoidosis (CS) is a granulomatous inflammation with patchy, multifocal infiltration of the pericardium, myocardium, and endocardium [72], its clinical presentation consists in atrio-ventricular blocks, ventricular arrhythmias (due to the disease's location in the left ventricle myocardial wall and intraventricular septum), sudden death, or heart failure symptoms [73,74].

These aspects make it essential to detect CS in individuals with extracardiac sarcoidosis as soon as possible to improve prognosis [75].

Despite the challenging diagnostic task, in all three major guidelines for diagnosis of CS such as American Thoracic society clinical practice for Sarcoidosis diagnosis [76], HRS expert consensus statement [77] and Japanese Ministry of Health and Welfare guidelines, CMR has a critical role to obtain an earlier diagnosis and a less severe stage of pathology [78]. LGE and LCE are generally seen in the mid-myocardium and sub-epicardium with a non-ischemic pattern, and both CMR and CCT can identify morphologic abnormalities and cardiac chamber functioning characteristics (LV and RV).

Iodinated contrast accumulates in the myocardial scar similarly to how gadolinium chelates do, which has led to an increasing number of studies showing imaging correlation between LCE CT) and LGE CMR imaging also in patients with cardiac sarcoidosis.

In particular, one of these studies by Aikawa et al. [79]demonstrates that in patients with or without implantable devices, LCE CT accurately determines the amount of fibrosis compared to LGE CMR.

Considering that implantable devices have a limited impact on the quality of images in LCE CT, such technique may become a new diagnostic tool for screening and monitoring of CS, especially in patients with contraindications to CMR. An example of patient with CS is reported in Fig. 4.

Moreover, it is possible to reconstruct the images of a CCT study with a larger field of view (FOV) in order to evaluate the lung parenchyma surrounding cardiac structures.

6.2.6. Amyloidosis

Amyloidosis is one of the causes of restrictive cardiomyopathy, which is characterized by ventricular filling impairment due to increased stiffness of the ventricle walls and loss of normal compliance: they don't release during the systole, obstructing cardiac chamber filling.

The buildup of insoluble amyloid fibrils in the myocardium results in conduction disorders and heart failure with intact ejection fraction.

Transthyretin cardiac amyloidosis (ATTR-CA) and immunoglobulin light chain cardiac amyloidosis (AL-CA) are the two subtypes of cardiac amyloidosis (CA) [80]. Two variants of the ATTR-CA are recognized: the ATTR wild type CA (ATTRwt-CA), also known as age-related CA, which is characterized by a normal transthyretin protein diffuse deposition, and the variant transthyretin CA (ATTRv-CA), also known as familial CA, which is linked to autosomal dominant inheritance [81].

For CA diagnosis the gold standard is an endomyocardial biopsy that is stained positively with Congo Red in ATTR-CA and a fat pad biopsy that confirms immunoglobulin light chain deposition in tandem with coherent cardiac imaging in AL-CA [82].

Another emerging non-invasive diagnostic method for ATTR-CA is bone nuclear scintigraphy with the use of nuclear radiotracers and interpretation using semiquantitative and quantitative scoring systems [83,84].

Concentric cardiac hypertrophy and an elevated E/e' ratio are hallmarks of transthoracic CA [6], and apical sparing using global longitudinal strain is another [85].

Cardiac magnetic resonance is extensively used to monitor and evaluate progression and patient response to therapy [86,87],

CMR in CA shows global subendocardial late gadolinium enhancement (LGE) and measure elevated ECV (mean 64 % n.v. 25–28 %).

The correlation between CMR findings and dual-energy cardiac computed tomography in cases of cardiac amyloidosis has been demonstrated in various studies in the last few years [88,89]. These studies used virtual monochromatic images at 50 KeV and iodine density mapping to demonstrate respectively global subendocardial enhancement with late iodine enhancement and elevated ECV [90].

Dual energy CT is suggested as a viable non-invasive diagnostic option in this instance as well, particularly for dialysis patients who have pacemakers or other monitoring devices, for whom CMR may be contraindicated.

6.2.7. Cardiac masses

Cardiac masses are rare in prevalence, but their characterization and differential diagnosis is essential for subsequent management. Usually, they are identified by echocardiography and CMR is the subsequent imaging method, but also CCT could be helpful as an alternative. In fact, CMR requires patient collaboration, is contraindicated among patients with implanted devices and may be limited in the evaluation of small mobile masses (due to limitation in spatial resolution). Moreover, CMR typically could not provide detailed imaging of coronary arteries when their relationship with the cardiac mass or their patency must be assessed to plan cardiac surgery [91,92].

Cardiac masses are usually categorized as neoplastic (both malignant and non-malignant) or non-neoplastic (or pseudo-tumors), such as cardiac thrombi or pericardial cysts.

Cardiac masses are usually benign, and the most frequent cardiac masses are pseudo-tumors, predominantly cardiac thrombi [92].

From a pragmatical point of view, one of the most frequent clinical clues is the distinction of cardiac thrombi. They can occur in all cardiac chambers, but most frequently are located leftward. They typically appear as a hypodense, low-attenuation filling defects and may be differentiated from neoplasms by investigation of predisposing risk factors, attachment location, shape, and type of mobility.

Left atrial appendage (LAA) thrombosis is strongly related to atrial fibrillation, but findings of low attenuation images in the LAA often might represents blood stasis, i.e. an incomplete mixing of contrast agent and blood. This "pseudo" filling defect could mimic a thrombus, especially in low-flow conditions and delayed imaging of the LAA can improve the specificity to distinguish between thrombus and circulatory stasis (e.g., a ratio between LAA and ascending aorta attenuation $\geq$0.75 HU at cardiac CT was associated with a 100 % negative predictive value for cardiac thrombi, while a ratio $<$0.75 has great sensitivity for detection of LAA thrombus and dense spontaneous echo-contrast at *trans*-esophageal echocardiographic examination) [93].

In order of predominance, benign primary cardiac tumors are usually represented by myxomas (at least 25–50 % of cases), lipomas and papillary fibroelastomas [91,92].

Cardiac myxomas are usually found in the left atrium in contiguity to the fossa ovalis, but could also be found in the right atrium, in the inferior vena cava, in both ventricles, and attached on the valve leaflets. Due to their usual location, they could lead to peripheral embolization or could prolapse across heart valves causing mechanical obstruction. On CCT, usually myxomas appear as hypodense ovoid masses and may demonstrate calcifications. The post-contrast enhancement can be heterogeneous, with variable intensity depending on the presence of intralesional necrosis or hemorrhage, and on the lesion's chronicity [91].

Cardiac lipomas are encapsulated tumors containing mature adipocytes and they may be found anywhere in the heart. Even though they are generally solitary lesions, multiple cardiac lipomas might occur (e.g., in patients with tuberous sclerosis). Approximately a half arise from the epicardial or mid-myocardial layers, while the other half are subendocardial, where they create filling defects with a homogenous appearance of fat attenuation (density $\leq$50 HU) [91].

Papillary fibroelastomas are solitary and small (average diameter 10 mm) non-calcified tumors which could arise from any endocardial surface, but the majority are attached on the aortic and mitral valves. Sometimes they are mobile masses, linked to the endocardium by a stalk and are prone to embolization or to mechanical interference with coronary ostia. Their usual appearance on CCT, is the one of a mobile hypodense mass with irregular borders with a thin stalk.

Among malignant neoplasms, the most frequent cardiac tumors are metastases, which are 20 to 40-fold more prevalent than primary cardiac tumors [91].

Cardiac metastases originate mostly from lung cancer (35–40 %), followed by breast (10 %) and hematologic (10–20 %) malignancies. Another tumor with high propensity to cardiac involvement is melanoma, usually in the late stages of the disease. Cardiac metastases involve mostly the pericardium (65–70 %), followed by epicardium (25–35 %) and myocardium (30 %), while endocardial or intracavitary involvement is rare. Pericardial metastasis might present as pericardial thickening, disruption, or effusion. Myocardial involvement usually appears as a thickening and with nodular aspect. Solid tumors frequently present post-contrast enhancement [91].

The most frequent malignant primary cardiac tumor is the angiosarcoma, which mostly originates from the right atrial free wall and consists of a large, multilobar mass spreading on the epicardial surface and replacing the right atrial wall, potentially involving the right coronary artery with the risk of rupture. At cardiac CT the angiosarcoma is usually characterized by the presence of a broad-based attachment to the right atrium that may be identified on early imaging. Delayed imaging permits a better visualization of the tumor on LCE images. The tumor is grossly hemorrhagic, and it often has a heterogeneous appearance because of scattered areas of non-enhancing necrosis. CT imaging may identify invasion of the nearby structures. The pericardial involvement usually has a "sheet-like" appearance due to the distribution and arrangement of tumor cells (while rabdomyosarcomas usually have a nodular appearance) [91].

6.2.8. Scar evaluation for catheter ablation procedures

Myocardial scar provides substrate of most of ventricular arrhythmias. Hence, in the last year, CMR became of crucial importance in the identification of myocardial scar in patients with ventricular arrhythmia based on its capability to define scar presence, site, segmental extent and its transmurality guiding the best electrophysiological procedure approach (endocardial vs epicardial)

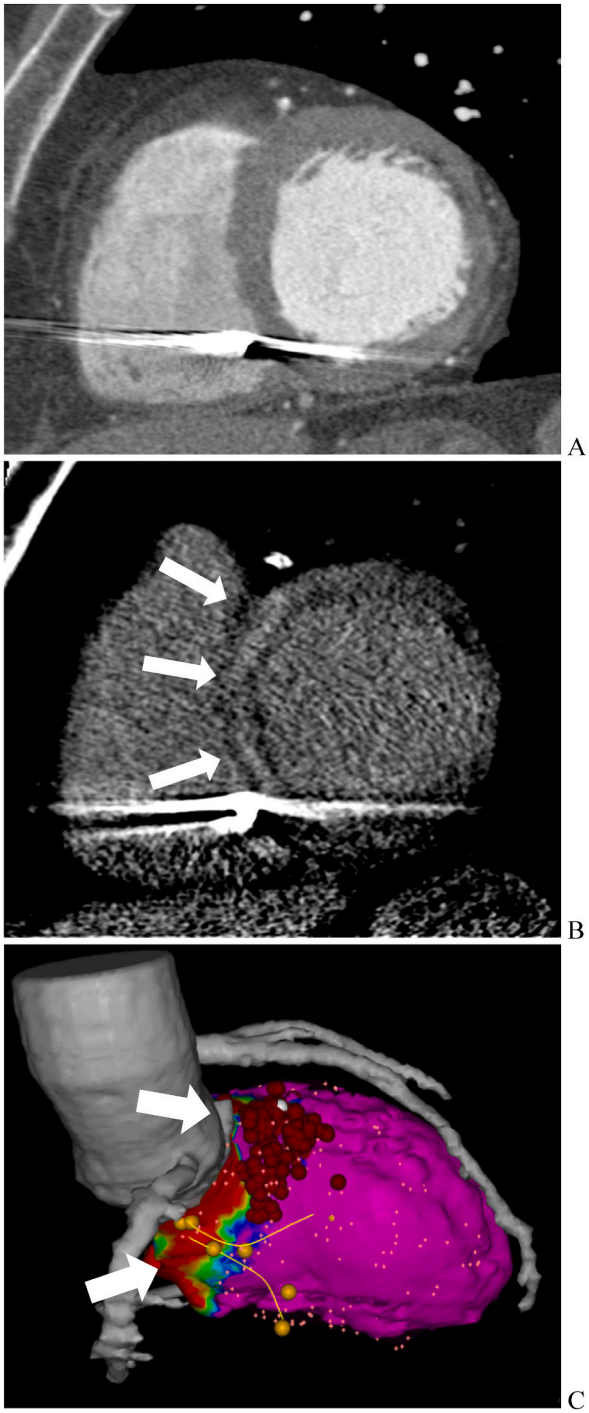

Fig. 6. Multiparametric CT including an angiographic scan (A) and a low voltage late contrast enhancement scan (B) in a patients with ICD suffering from recurrent ventricular tachycardia. Myocardial wall thickness resulted preserved in CTA (A) while LCE-CT showed a mesocardial scar (white arrows in B) involving the basal interventricular septum. The streaks artifact from ICD minimally interfered with the assessment of scar in the posterior septum. Electroanatomic mapping obtained with an endocardial approach (C) confirmed low voltages in the basal septum (red area with white arrows in C) corresponding to scar identified by LCE-CT, hence ablation was successfully performed on the border zone of that area (red dots in C). (For interpretation of the references to color in this figure legend, the reader is referred to the Web version of this article.)

improving catheter ablation procedural time and success [94]. Unfortunately, often patients candidate to catheter ablation procedure had an implantable cardioverter defibrillator (ICD) which significantly limited myocardial assess ability for artifacts related to the ICD's pulse generator [95]. Therefore, alternative strategies based on CCT has been developed. In fact, ICD minimally interfere with myocardial visualization on CT, with artifacts related to shock coils affecting less than 2 % of myocardial wall [23] associated to the advantages of rapid acquisition times and superior spatial resolution. In patients affected by ischemic cardiomyopathy a myocardial wall thickness (WT) < 5 mm was proposed to distinguish scarred from healthy myocardium [96] however it failed in distinguishing 36 % of patients with subendocardial scar comparted to LGE-CMR [97] and showed a global sensitivity for detection of arrhytmogenic channels and channel entrances of 61.8 % and 33.1 %, respectively [97]. Additionally, this approach is not able to identify non-ischemic scar, typically with mesocardial or subepicardial scar, with poor correlation with low voltages suggestive of scar at electroanatomic mapping (EAM) with 13 ± 16 % agreement according to Yamashita et al. [98] The identification of myocardial scar in cardiac CT though the acquisition of a delayed scan the so called "late iodine or contrast enhancement scan" (LIE or LCE) has the potential to overcome all the aforementioned limitation, in fact LCE-CCT had excellent agreement with LGE-MRI [21] and also with low voltages and late potential at EAM [23] regardless scar etiology and transmurality and with better performance than the assessment of wall thinning [23]. In particular, Esposito et al. found that compared low voltages, LCE-CCT good sensitivity (76 %), good specificity (86 %), and very high negative predictive value (95 %). Late potentials and RF ablation points fell on scarred segments identified from LCE-CCT in 79 % and 81 % of cases, respectively [23]. Good results of these approach were recently confirmed by Conte et al. showing a diagnostic accuracy of LCE-CT in the identification of scarred myocardium compared to EAM of 94.1 % on a per-segment basis [99].

The isotropic volume and the high spatial resolution lead also to the possibility to integrate scar information from LCE-CCT to anatomic information from angiographic scan as coronary artery course, cardiac chamber anatomy, epicardial fat in order to produce a 3D model including both information for live guidance of ablation procedure [23].

Additionally, the high spatial resolution allows the application of radiomic analysis of LCE scan, improving the capability to characterize myocardial susceptibility to ventricular arrhythmia by the evaluation of LCE heterogeneity, representative of interstitial fibrosis heterogeneous distribution, which resulted associated to different patterns of structural remodeling related to different etiology of recurrent ventricular tachycardia [63]. An example of multiparametric LCE-CCT before an ablation procedure and fusion imaging with electroanatomic mapping is reported in Fig. 6.

LCE-CCT based detection of arrhythmia substrate could be also useful for planning of stereotactic radio-ablation which is recently introduced as potential treatment alternative for high procedural risk patients [100]. On the other hand, CCT cannot provide information about the presence of edema in post-myocarditis patients, which is of crucial importance for correct clinical management; at this aim recent study suggested the possibility to merge LCE-CCT images with FDG-PET in order to integrated structural to function information about myocardial scar substrates of ventricular arrhythmia [17].

7. Advantages and disadvantages of late contrast enhancement CT compared to cardiac magnetic resonance

CCT imaging exposes the patients to ionizing radiation and nephrotoxic contrast agents compared to CMR which is a radiation-free exam and gadolinium-based contrast agents do not cause acute kidney injury. So, in order to avoid the risk of acute kidney injury the patients renal function must be evaluated by measuring serum creatinine values and glomerular filtration rate [101]. Moreover, in order to minimize the risk of allergic reactions to CT contrast, it is important to assess the anamnestic data of previous allergic reactions to iodine contrast medium and/or history of anaphylaxis, thus adopting the necessary pre-medication [102].

The contrast-noise-ratio (CNR) on LCE imaging is less favorable compared to CMR LGE [22] and the correct interpretation of LCE images is more dependent on radiologist's experience compared to LGE, however experienced readers may identify myocardial scars on both LCE and LGE images with similar diagnostic accuracy [21].

Moreover, the gold standard for cardiac tissue characterization is still CMR with quantitative T1 and T2 mapping and LGE imaging and, to date, CT technology does not allow to obtain the information provided by mapping imaging.

Despite these limitations LCE imaging seems to be a promising and feasible alternative to CMR for comprehensive cardiac evaluation in the emergency setting, as MR scanners are rarely present in emergency departments while CT scanner capable of ECG-gated acquisition are more widely available. Moreover, CT may be a feasible alternative to CMR for patients with implanted devices as CT is less prone to artifacts compared to CMR [23], and for patients with limited compliance that may be unable to complete a comprehensive CMR examination.

A comprehensive CCT protocol may represent an excellent one-stop-shop exam for patient with acute thoracic pain in the emergency setting due to the possibility to rule out conditions such as obstructive CAD, acute aortic syndromes and pulmonary embolism and to evaluate the presence if myocardial LCE and ECV [22].

With current state-of-the-art CT scanners LCE images results in a negligible increase in radiation dose compared to older-generation hardware [22].

8. The future: photon counting

While precedent studies have shown good agreement between CCT-derived ECV values and its CMR equivalent, its measurement has relied on a subtraction-derived method, requiring manually drawing regions of interest (ROIs) on left ventricular myocardium and the blood pool, then correcting the map for hematocrit [25–27], a time-consuming process.

Dual energy CTs (DECT), thanks to their ability to spectrally discriminate between high and low energy photons, have introduced

the possibility of direct mapping iodine density on late enhancement scans, making automatic ECV evaluation feasible in a time-constrained routine clinical workflow (LCE-DECT); the literature corroborates LCE-DECT usage on the field as being on par, or exceeding, traditional subtraction derived ECV-CCT in consistency and accuracy [103].

Photon counting CT technology (PCCT) promises further improvements [104], especially on spectral discrimination over DECT [104] and thus greatly reducing beam hardening artifacts. The higher and improved contrast-to-noise ratio provides dose reduction capabilities, a very appreciated side-feature in cardiovascular imaging [105–108]. Its smaller detector elements provide higher spatial resolution and a reduction of bloom artifacts [109–111]. Recent works have already demonstrated the feasibility in clinical practice to reduce contrast medium dose in CCTA with PCCT [112] and to evaluate ECV and myocardial scar on LCE acquisitions [113].

PCCT may improve quantitative imaging thanks to unlocking the possibility of using contrast medium other than iodine agents, such as gadolinium, barium or gold. One immediate benefit consists in enabling CT quantitative imaging in patients barred from iodine contrast medium exposition. Another benefit may be the potential application of administering different contrast agent at the same time and separately mapping their different specific distribution, which may provide additional quantitative imaging information [114,115].

Still, PCCT systems are particularly susceptible to cross-talk artifacts due to their reduced detector element size [116]. A smaller detector element size leads to more split-border photons being detected, and a smaller distance between elements leads to second-order fluorescence photons, born in adjacent elements, being detected more often. Moreover, fast detector elements are required in order to minimize charge sharing and pulse pileup problems, even though the resulting photon miscount may be circumvented by clever work-arounds such as trained neural-networks [117].

A study by Becker et al. [118] attests to overall better image quality and improved signal-to-noise ratio in the field of abdominal imaging, while Risch et al. provides an initial quantitative cardiac imaging application for estimating epicardial adipose tissue [119]. Recent literature has confirmed that PCCT has the potential to provide unprecedented image quality in vascular and cardiovascular imaging while reducing the burden of radiation to which patients are exposed, contrast medium doses and providing higher diagnostic accuracy [120–122].

9. Conclusions

Technological improvement in CT scanners have increased the diagnostic possibilities of such technique which represents today a truly multiparametric cardiac exam with a very wide range of indications and applications. The emerging role of LCE imaging and CT derived ECV may allow cardiac tissue characterization in patient to whom CMR may be precluded due to long waiting lists or because they have poor compliance, claustrophobia or have MR-unsafe implanted devices.

Funding statement

No funding was received for this work.

Data availability statement

N/A.

Declaration of interest's statement

The authors declare the following financial interests/personal relationships which may be considered as potential competing interests: Marco Gatti MD is a Guest editor for Heliyon Clinical Research.

CRediT authorship contribution statement

Davide Tore: Writing – review & editing, Conceptualization. **Riccardo Faletti:** Writing – review & editing, Conceptualization. **Anna Palmisano:** Writing – review & editing, Conceptualization. **Sara Salto:** Writing – original draft. **Katia Rocco:** Writing – original draft. **Ambra Santonocito:** Writing – original draft. **Clara Gaetani:** Writing – original draft. **Andrea Biondo:** Writing – original draft. **Elena Bozzo:** Writing – original draft. **Fabio Giorgino:** Writing – original draft. **Ilenia Landolfi:** Writing – original draft. **Francesca Menchini:** Writing – original draft. **Antonio Esposito:** Writing – review & editing, Conceptualization. **Paolo Fonio:** Writing – review & editing, Conceptualization. **Marco Gatti:** Writing – review & editing, Conceptualization.

Declaration of competing interest

The authors declare the following financial interests/personal relationships which may be considered as potential competing interests:Dr. Marco Gatti is an Editor for Heliyon. If there are other authors, they declare that they have no known competing financial interests or personal relationships that could have appeared to influence the work reported in this paper.

References

[1] G.A. Rodriguez-Granillo, Delayed enhancement cardiac computed tomography for the assessment of myocardial infarction: from bench to bedside, Cardiovasc. Diagn. Ther. 7 (2017) 159–170.
[2] C.B. Higgins, P.L. Hagen, J.D. Newell, W.S. Schmidt, F.H. Haigler, Contrast Enhancement of Myocardial Infarction: Dependence on Necrosis and Residual Blood Flow and the Relationship to Distribution of Scintigraphic Imaging Agents, 1982.
[3] P.T. Siemers, C.B. Higgins, W. Schmidt, W. Ashburn, P. Detection Hagan, Quantitation and contrast enhancement of myocardial infarction utilizing computerized axial tomography: comparison with histochemical staining and 99mTc-pyrophosphate imaging, Invest. Radiol. 13 (2) (1977) 103–109.
[4] P.W. Doherty, M.J. Lipton, W.H. Berninger, C.G. Skioldebrand, E. Carlsson, R.W. Redington, Detection and Quantitation of Myocardial Infarction in Vivo Using Transmission Computed Tomography, 1981.
[5] M.T. McNamara, C.B. Higgins, R.L. Ehman, D. Revel, R. Sievers, B.C. Robert Brasch, MAGNETIC RESONANCE Acute Myocardial Ischemia: Magnetic Resonance Contrast Enhancement with Gadolinium-DTPA1, 1984.
[6] D. Tscholakoff, C.B. Higgins, U. Sechtem, M.T. McNamara, Occlusive and Reperfused Myocardial Infarcts: Effect of Gd-DTPA on ECG-Gated MR Imaging, 1986.
[7] M. Saeed, M.F. Wendland, Y. Takehara, C.B. Higgins, Reversible and Irreversible Injury in the Reperfused Myocardium: Differentiation with Contrast Material-Enhanced MR Imaging, 1990.
[8] M. Saeed, G. Lund, M.F. Wendland, J. Bremerich, Hanns-Joachim Weinmann, C.B. Higgins, Magnetic Resonance Characterization of the Peri-Infarction Zone of Reperfused Myocardial Infarction with Necrosis-specific and Extracellular Nonspecific Contrast Media, 2001.
[9] A. De Roos, A.C. van Rossum, E. van der Wall, S. Postema, J. Doornbos, N. Matheijssen, P.R.M. van Dijkman, F.C. Visser, AE van Voorthuisen, Reperfused and nonreperfused myocardial infarction, Diagnostic Potential of Gd-DTPA-Enhanced MR, Imaging 172 (3) (1989) 717–720.
[10] H.W. Eichstaedt, R. Felix, F.C. Dougherty, M. Langer, W. Rutsch, H. Schmutzler, Magnetic resonance imaging (MRI) in different stages of myocardial infarction using the contrast agent gadolinium-DTPA, Clin. Cardiol. 9 (1986) 527–535, https://doi.org/10.1002/clc.4960091102.
[11] R.H. Chan, B.J. Maron, I. Olivotto, M.J. Pencina, G.E. Assenza, T. Haas, J.R. Lesser, C. Gruner, A.M. Crean, H. Rakowski, et al., Prognostic value of quantitative contrast-enhanced cardiovascular magnetic resonance for the evaluation of sudden death risk in patients with hypertrophic cardiomyopathy, Circulation 130 (2014) 484–495, https://doi.org/10.1161/CIRCULATIONAHA.113.007094.
[12] T.J. Stocker, S. Deseive, J. Leipsic, M. Hadamitzky, M.Y. Chen, R. Rubinshtein, M. Heckner, J.J. Bax, X.M. Fang, E.L. Grove, et al., Reduction in radiation exposure in cardiovascular computed tomography imaging: results from the PROspective multicenter registry on RadiaTion dose estimates of cardiac CT AngIOgraphy iN daily practice in 2017 (PROTECTION VI), Eur. Heart J. 39 (2018) 3715–3723.
[13] B.L. Gerber, B. Belge, G.J. Legros, P. Lim, A. Poncelet, A. Pasquet, G. Gisellu, E. Coche, J.L.J. Vanoverschelde, Characterization of acute and chronic myocardial infarcts by multidetector computed tomography: comparison with contrast-enhanced magnetic resonance, Circulation 113 (2006) 823–833, https://doi.org/10.1161/CIRCULATIONAHA.104.529511.
[14] T. Aikawa, N. Oyama-Manabe, M. Naya, H. Ohira, A. Sugimoto, I. Tsujino, M. Obara, O. Manabe, K. Kudo, H. Tsutsui, et al., Delayed contrast-enhanced computed tomography in patients with known or suspected cardiac sarcoidosis: a feasibility study, Eur. Radiol. 27 (2017) 4054–4063, https://doi.org/10.1007/s00330-017-4824-x.
[15] Y. Tanabe, T. Kido, A. Kurata, T. Kouchi, N. Fukuyama, T. Yokoi, T. Uetani, N. Yamashita, M. Miyagawa, T. Mochizuki, Late iodine enhancement computed tomography with image subtraction for assessment of myocardial infarction, Eur. Radiol. 28 (2018) 1285–1292, https://doi.org/10.1007/s00330-017-5048-9.
[16] L. Zhao, X. Ma, M.C. Delano, T. Jiang, C. Zhang, Y. Liu, Z. Zhang, Assessment of myocardial fibrosis and coronary arteries in hypertrophic cardiomyopathy using combined arterial and delayed enhanced CT: comparison with MR and coronary angiography, Eur. Radiol. 23 (2013) 1034–1043, https://doi.org/10.1007/s00330-012-2674-0.
[17] A. Palmisano, D. Vignale, G. Peretto, E. Busnardo, C. Calcagno, C. Campochiaro, G. De Luca, S. Sala, P. Ferro, C. Basso, et al., Hybrid FDG-PET/MR or FDG-PET/CT to detect disease activity in patients with persisting arrhythmias after myocarditis, JACC Cardiovasc Imaging 14 (2021) 288–292, https://doi.org/10.1016/j.jcmg.2020.03.009.
[18] Wendland, M.F.; Saeed, M.; Arheden, H.; Gao, D.-W.; Canet, E.; Bremerich, J.; Dae, M.W.; Higgins, C.B. Toward Necrotic Cell Fraction Measurement by Contrast-Enhanced MRI of Reperfused Ischemically Injured Myocardium,.
[19] Arheden, H.; Saeed, M.; Higgins, C.B.; Gao, D.-W.; Bremerich, J.; Wyttenbach, R.; Dae, M.W.; Wendland, M.F. Measurement of the Distribution Volume of Gadopentetate Dimeglumine at Echo-Planar MR Imaging to Quantify Myocardial Infarction: Comparison with 99m Tc-DTPA Autoradiography in Rats 1;.
[20] K.G. Ordovas, C.B. Higgins, Delayed contrast enhancement on MR images of myocardium: past, present, future, Radiology 261 (2011) 358–374.
[21] A. Palmisano, D. Vignale, G. Benedetti, A. Del Maschio, F. De Cobelli, A. Esposito, Late iodine enhancement cardiac computed tomography for detection of myocardial scars: impact of experience in the clinical practice, Radiologia Medica 125 (2020) 128–136, https://doi.org/10.1007/s11547-019-01108-7.
[22] A. Palmisano, D. Vignale, M. Tadic, F. Moroni, D. de Stefano, M. Gatti, E. Boccia, R. Faletti, M. Oppizzi, G. Peretto, et al., Myocardial late contrast enhancement CT in troponin-positive acute chest pain syndrome, Radiology (2021), https://doi.org/10.1148/radiol.211288.
[23] A. Esposito, A. Palmisano, S. Antunes, G. Maccabelli, C. Colantoni, P.M.V. Rancoita, F. Baratto, C. Di Serio, G. Rizzo, F. De Cobelli, et al., Cardiac CT with delayed enhancement in the characterization of ventricular tachycardia structural substrate: relationship between CT-segmented scar and electro-anatomic mapping, JACC Cardiovasc Imaging 9 (2016) 822–832, https://doi.org/10.1016/j.jcmg.2015.10.024.
[24] P. Haaf, P. Garg, D.R. Messroghli, D.A. Broadbent, J.P. Greenwood, S. Plein, Cardiac T1 mapping and extracellular volume (ECV) in clinical practice: a comprehensive review, J. Cardiovasc. Magn. Reson. 18 (2016).
[25] A.F. Abadia, M. van Assen, S.S. Martin, V. Vingiani, L.P. Griffith, D.A. Giovagnoli, M.J. Bauer, U.J. Schoepf, Myocardial extracellular volume fraction to differentiate healthy from cardiomyopathic myocardium using dual-source dual-energy CT, J Cardiovasc Comput Tomogr 14 (2020) 162–167, https://doi.org/10.1016/j.jcct.2019.09.008.
[26] D. Han, B. Tamarappoo, E. Klein, J. Tyler, T. Chakravarty, Y. Otaki, R. Miller, E. Eisenberg, R. Park, S. Singh, et al., Computed tomography angiography-derived extracellular volume fraction predicts early recovery of left ventricular systolic function after transcatheter aortic valve replacement, Eur Heart J Cardiovasc Imaging 22 (2021) 179–185, https://doi.org/10.1093/ehjci/jeaa310.
[27] T.A. Treibel, S. Bandula, M. Fontana, S.K. White, J.A. Gilbertson, A.S. Herrey, J.D. Gillmore, S. Punwani, P.N. Hawkins, S.A. Taylor, et al., Extracellular volume quantification by dynamic equilibrium cardiac computed tomography in cardiac amyloidosis, J Cardiovasc Comput Tomogr 9 (2015) 585–592, https://doi.org/10.1016/j.jcct.2015.07.001.
[28] U.K. Radunski, G.K. Lund, C. Stehning, B. Schnackenburg, S. Bohnen, G. Adam, S. Blankenberg, K. Muellerleile, CMR in patients with severe myocarditis: diagnostic value of quantitative tissue markers including extracellular volume imaging, JACC Cardiovasc Imaging 7 (2014) 667–675, https://doi.org/10.1016/j.jcmg.2014.02.005.
[29] P. Garg, D.A. Broadbent, P.P. Swoboda, J.R.J. Foley, G.J. Fent, T.A. Musa, D.P. Ripley, B. Erhayiem, L.E. Dobson, A.K. McDiarmid, et al., Acute infarct extracellular volume mapping to quantify myocardial area at risk and chronic infarct size on cardiovascular magnetic resonance imaging, Circ Cardiovasc Imaging 10 (2017), https://doi.org/10.1161/CIRCIMAGING.117.006182.
[30] P.R. Scully, G. Bastarrika, J.C. Moon, T.A. Treibel, Myocardial extracellular volume quantification by cardiovascular magnetic resonance and computed tomography, Curr. Cardiol. Rep. 20 (2018).
[31] N. Mewton, C.Y. Liu, P. Croisille, D. Bluemke, J.A.C. Lima, Assessment of myocardial fibrosis with cardiovascular magnetic resonance, J. Am. Coll. Cardiol. 57 (2011) 891–903.
[32] J. Vogel-Claussen, C.E. Rochitte, K.C. Wu, I.R. Kamel, T.K. Foo, J.A.C. Lima, D.A. Bluemke, Delayed enhancement MR imaging: utility in myocardial assessment, Radiographics 26 (2006) 795–810.
[33] K.R. Anderson, M.G. Sutton, J.T. Lie, Histopathological types of cardiac fibrosis in myocardial disease, J. Pathol. 128 (1979) 79–85.
[34] K. yue Diao, Z. gang Yang, H. yan Xu, X. Liu, Q. Zhang, K. Shi, L. Jiang, L. Xie, Wen L. yi jun, Y. Guo, Kun histologic validation of myocardial fibrosis measured by T1 mapping: a systematic review and meta-analysis, J. Cardiovasc. Magn. Reson. 18 (2016) 1–11, https://doi.org/10.1186/s12968-016-0313-7.

[35] M.S. Nacif, N. Kawel, J.J. Lee, X. Chen, J. Yao, A. Zavodni, C.T. Sibley, J.A.C. Lima, S. Liu, D.A. Bluemke, Interstitial myocardial fibrosis assessed as extracellular volume fraction with low-radiation-dose cardiac CT, Radiology 264 (2012) 876–883, https://doi.org/10.1148/radiol.12112458.

[36] D.R. Messroghli, J.C. Moon, V.M. Ferreira, L. Grosse-Wortmann, T. He, P. Kellman, J. Mascherbauer, R. Nezafat, M. Salerno, E.B. Schelbert, et al., Clinical recommendations for cardiovascular magnetic resonance mapping of T1, T2, T2 and extracellular volume: a consensus statement by the society for cardiovascular magnetic resonance (SCMR) endorsed by the European association for cardiovascular imaging (eacvi), J. Cardiovasc. Magn. Reson. 19 (2017).

[37] R.J. Kim, T.S.E. Albert, J.H. Wible, M.D. Elliott, J.C. Allen, J.C. Lee, M. Parker, A. Napoli, R.M. Judd, Performance of delayed-enhancement magnetic resonance imaging with gadoversetamide contrast for the detection and assessment of myocardial infarction : an international, multicenter, double-blinded, randomized trial, Circulation 117 (2008) 629–637, https://doi.org/10.1161/CIRCULATIONAHA.107.723262.

[38] M.S. Nacif, N. Kawel, J.J. Lee, X. Chen, J. Yao, A. Zavodni, C.T. Sibley, J.A.C. Lima, S. Liu, D.A. Bluemke, Interstitial myocardial fibrosis assessed as extracellular volume fraction with low-radiation-dose cardiac CT, Radiology 264 (2012) 876–883, https://doi.org/10.1148/radiol.12112458.

[39] H.J. Lee, D.J. Im, J.C. Youn, S. Chang, Y.J. Suh, Y.J. Hong, Y.J. Kim, J. Hur, B.W. Choi, Myocardial extracellular volume fraction with dual-energy equilibrium contrast-enhanced cardiac ct in nonischemic cardiomyopathy: a prospective comparison with cardiac MR imaging, Radiology 280 (2016) 49–57, https://doi.org/10.1148/radiol.2016151289.

[40] H.J. Lee, D.J. Im, J.C. Youn, S. Chang, Y.J. Suh, Y.J. Hong, Y.J. Kim, J. Hur, B.W. Choi, Myocardial extracellular volume fraction with dual-energy equilibrium contrast-enhanced cardiac ct in nonischemic cardiomyopathy: a prospective comparison with cardiac MR imaging, Radiology 280 (2016) 49–57, https://doi.org/10.1148/radiol.2016151289.

[41] Y. Jin Hong, T. Kyung Kim, D. Hong, C. Hwan Park, S. Jong Yoo, M. Ellen Wickum, J. Hur, H.-J. Lee, Y. Jin Kim, Y. Joo Suh, et al., Myocardial characterization using dual-energy CT in doxorubicin-induced DCM comparison with CMR T1-mapping and histology in a rabbit model, JACC (J. Am. Coll. Cardiol.): Cardiovasc Imaging (2016) 836–845.

[42] A.S. Fahmy, E.J. Rowin, R.H. Chan, W.J. Manning, M.S. Maron, R. Nezafat, Improved quantification of myocardium scar in late gadolinium enhancement images: deep learning based image fusion approach, J. Magn. Reson. Imag. 54 (2021) 303–312, https://doi.org/10.1002/jmri.27555.

[43] P.H. Kee, D. Danila, CT imaging of myocardial scar burden with CNA35-conjugated gold nanoparticles, Nanomedicine 14 (2018) 1941–1947, https://doi.org/10.1016/j.nano.2018.06.003.

[44] K. Thygesen, J.S. Alpert, A.S. Jaffe, B.R. Chaitman, J.J. Bax, D.A. Morrow, H.D. White, Fourth universal definition of myocardial infarction (2018), J. Am. Coll. Cardiol. 72 (2018) 2231–2264, https://doi.org/10.1016/j.jacc.2018.08.1038.

[45] F. Torchio, A. Garatti, D. Ronco, M. Matteucci, G. Massimi, R. Lorusso, Left ventricular pseudoaneurysm: the niche of post-infarction mechanical complications, Ann. Cardiothorac. Surg. 11 (2022) 290–298, https://doi.org/10.21037/acs-2022-ami-25.

[46] J. El ouazzani, I. Jandou, Aneurysm and pseudoaneurysm of the left ventricle, Annals of Medicine and Surgery 75 (2022).

[47] A.G. Iosifescu, T.A. Iosifescu, A.T. Timisescu, E.L. Antohi, V.A. Iliescu, Left ventricular pseudoaneurysms discovered early after acute myocardial infarction: the surgical timing dilemma, Tex. Heart Inst. J. 49 (2022), https://doi.org/10.14503/THIJ-20-7462.

[48] E.M. Bertrand Fikahem, O.-O. Franck Hardain, M.-N. Flore Solange, K.L. Christian Michel, G. Thierry Raoul, K.-K. Suzy-Gisèle, Left ventricle pseudoaneurysm: contribution of multimodality imaging to the diagnosis, Case Rep Cardiol 2014 (2014) 1–4, https://doi.org/10.1155/2014/531929.

[49] R.W. Bauer, J.M. Kerl, N. Fischer, T. Burkhard, M.C. Larson, H. Ackermann, T.J. Vogl, Dual-energy CT for the assessment of chronic myocardial infarction in patients with chronic coronary artery disease: comparison with 3-T MRI, Am. J. Roentgenol. 195 (2010) 639–646, https://doi.org/10.2214/AJR.09.3849.

[50] T.A. Treibel, M. Fontana, J.A. Steeden, A. Nasis, J. Yeung, S.K. White, S. Sivarajan, S. Punwani, F. Pugliese, S.A. Taylor, et al., Automatic quantification of the myocardial extracellular volume by cardiac computed tomography: synthetic ECV by CCT, J Cardiovasc Comput Tomogr 11 (2017) 221–226, https://doi.org/10.1016/j.jcct.2017.02.006.

[51] S.M. Ko, S.H. Hwang, H.J. Lee, Role of cardiac computed tomography in the diagnosis of left ventricular myocardial diseases, J Cardiovasc Imaging 27 (2019) 73–92.

[52] L. La Grutta, P. Toia, E. Maffei, F. Cademartiri, R. Lagalla, M. Midiri, Infarct characterization using CT, Cardiovasc. Diagn. Ther. 7 (2017) 171–188.

[53] A.L.P. Caforio, S. Pankuweit, E. Arbustini, C. Basso, J. Gimeno-Blanes, S.B. Felix, M. Fu, T. Heliö, S. Heymans, R. Jahns, et al., Current state of knowledge on aetiology, diagnosis, management, and therapy of myocarditis: a position statement of the European society of cardiology working group on myocardial and pericardial diseases, Eur. Heart J. 34 (2013) 2636–2648, https://doi.org/10.1093/eurheartj/eht210.

[54] S. Oda, T. Emoto, T. Nakaura, M. Kidoh, D. Utsunomiya, Y. Funama, Y. Nagayama, S. Takashio, M. Ueda, T. Yamashita, et al., Myocardial late iodine enhancement and extracellular volume quantification with dual-layer spectral detector dual-energy cardiac ct, Radiol Cardiothorac Imaging 1 (2019), https://doi.org/10.1148/ryct.2019180003.

[55] G. Dambrin, J.P. Laissy, J.M. Serfaty, C. Caussin, B. Lancelin, J.F. Paul, Diagnostic value of ECG-gated multidetector computed tomography in the early phase of suspected acute myocarditis. A preliminary comparative study with cardiac MRI, Eur. Radiol. 17 (2007) 331–338, https://doi.org/10.1007/s00330-006-0391-2.

[56] K. Axsom, F. Lin, J.W. Weinsaft, J.K. Min, Evaluation of myocarditis with delayed-enhancement computed tomography, J Cardiovasc Comput Tomogr 3 (2009) 409–411, https://doi.org/10.1016/j.jcct.2009.09.003.

[57] J.R. Ghadri, K. Kato, V.L. Cammann, S. Gili, S. Jurisic, D. Di Vece, A. Candreva, K.J. Ding, J. Micek, K.A. Szawan, et al., Long-term prognosis of patients with Takotsubo syndrome, J. Am. Coll. Cardiol. 72 (2018) 874–882, https://doi.org/10.1016/j.jacc.2018.06.016.

[58] W. Desmet, J. Bennett, B. Ferdinande, D. deCock, T. Adriaenssens, M. Coosemans, P. Sinnaeve, P. Kayaert, C. Dubois, The apical nipple sign: a useful tool for discriminating between anterior infarction and transient left ventricular ballooning syndrome, Eur Heart J Acute Cardiovasc Care 3 (2014) 264–267, https://doi.org/10.1177/2048872613517359.

[59] J. Roncalli, D. Carrie, J.M. Fauvel, D.W.A. Losordo, "Hawk's beak" to identify the new transient midventricular tako-tsubo syndrome, Int. J. Cardiol. 127 (2008), https://doi.org/10.1016/j.ijcard.2007.04.140.

[60] D. Sueta, S. Oda, Y. Izumiya, K. Kaikita, M. Kidoh, D. Utsunomiya, Y. Yamashita, K. Tsujita, Comprehensive assessment of Takotsubo cardiomyopathy by cardiac computed tomography, Emerg. Radiol. 26 (2019) 109–112, https://doi.org/10.1007/s10140-018-1610-2.

[61] R. Citro, H. Okura, J.R. Ghadri, C. Izumi, P. Meimoun, M. Izumo, D. Dawson, S. Kaji, I. Eitel, N. Kagiyama, et al., Multimodality imaging in Takotsubo syndrome: a joint consensus document of the European association of cardiovascular imaging (EACVI) and the Japanese society of echocardiography (JSE), J. Echocardiogr. 18 (2020) 199–224, https://doi.org/10.1007/s12574-020-00480-y.

[62] P.G. Masci, A. Barison, G.D. Aquaro, A. Pingitore, R. Mariotti, A. Balbarini, C. Passino, M. Lombardi, M. Emdin, Myocardial delayed enhancement in paucisymptomatic nonischemic dilated cardiomyopathy, Int. J. Cardiol. 157 (2012) 43–47, https://doi.org/10.1016/j.ijcard.2010.11.005.

[63] A. Esposito, A. Palmisano, S. Antunes, C. Colantoni, P.M.V. Rancoita, D. Vignale, F. Baratto, P. Della Bella, A. Del Maschio, F. De Cobelli, Assessment of remote myocardium heterogeneity in patients with ventricular tachycardia using texture analysis of late iodine enhancement (LIE) cardiac computed tomography (CCT) images, Mol Imaging Biol 20 (2018) 816–825, https://doi.org/10.1007/s11307-018-1175-1.

[64] Y. Ohta, J. Kishimoto, S. Kitao, H. Yunaga, N. Mukai-Yatagai, S. Fujii, K. Yamamoto, T. Fukuda, T. Ogawa, Investigation of myocardial extracellular volume fraction in heart failure patients using iodine map with rapid-KV switching dual-energy CT: segmental comparison with MRI T1 mapping, J Cardiovasc Comput Tomogr 14 (2020) 349–355, https://doi.org/10.1016/j.jcct.2019.12.032.

[65] Y. Ohta, S. Kitao, H. Yunaga, T. Watanabe, N. Mukai—Yatagai, J. Kishimoto, K. Yamamoto, T. Ogawa, Quantitative evaluation of non-ischemic dilated cardiomyopathy by late iodine enhancement using rapid KV switching dual-energy computed tomography: a feasibility study, J Cardiovasc Comput Tomogr 13 (2019) 148–156, https://doi.org/10.1016/j.jcct.2018.10.028.

[66] P.J. Sparrow, N. Merchant, Y.L. Provost, D.J. Doyle, E.T. Nguyen, N.S. Paul, CT and MR imaging findings in patients with acquired heart disease at risk for sudden cardiac death, Radiographics 29 (2009) 805–823, https://doi.org/10.1148/rg.293085715.

[67] S.M. Ko, T.H. Kim, E.J. Chun, J.Y. Kim, S.H. Hwang, Assessment of left ventricular myocardial diseases with cardiac computed tomography, Korean J. Radiol. 20 (2019) 333–351, https://doi.org/10.3348/kjr.2018.0280.

[68] C. Langer, M. Both, H. Harders, M. Lutz, M. Eden, C. Kühl, B. Sattler, O. Jansen, P. Schaefer, N. Frey, Late enhanced computed tomography in hypertrophic cardiomyopathy enables accurate left-ventricular volumetry, Eur. Radiol. 25 (2015) 575–584, https://doi.org/10.1007/s00330-014-3434-0.

[69] C. Langer, M. Lutz, M. Eden, M. Lüdde, M. Hohnhorst, C. Gierloff, M. Both, W. Burchert, L. Faber, D. Horstkotte, et al., Hypertrophic cardiomyopathy in cardiac CT: a validation study on the detection of intramyocardial fibrosis in consecutive patients, Int. J. Cardiovasc. Imag. 30 (2014) 659–667, https://doi.org/10.1007/s10554-013-0358-8.

[70] H.I. Litt, Dual-energy (spectral) late iodine enhancement cardiac ct: does a dual-layer detector make it work? Radiol Cardiothorac Imaging 1 (2019).

[71] E. Markatis, A. Afthinos, E. Antonakis, I.C. Papanikolaou, Cardiac sarcoidosis: diagnosis and management, Rev. Cardiovasc. Med. 21 (2020) 321–338.

[72] W.C. Roberts, M.A. Hugh Mcallister, J Ferrans Victor, D. C, Sarcoidosis of the Heart: A Clinicopathologic Study of 35 Necropsy Patients (Group I) and Review of 78 Previously Described Necropsy Patients (Group II) 83 (1977).

[73] D.H. Birnie, P.B. Nery, A.C. Ha, R.S.B. Beanlands, Cardiac Sarcoidosis, 2016.

[74] F. Terasaki, A. Azuma, T. Anzai, N. Ishizaka, Y. Ishida, M. Isobe, T. Inomata, H. Ishibashi-Ueda, Y. Eishi, M. Kitakaze, et al., JCS 2016 guideline on diagnosis and treatment of cardiac sarcoidosis – digest version, Circ. J. 83 (2019) 2329–2388.

[75] S.W. Dubrey, R.H. Falk, Diagnosis and management of cardiac sarcoidosis, Prog. Cardiovasc. Dis. 52 (2010) 336–346, https://doi.org/10.1016/j.pcad.2009.11.010.

[76] E.D. Crouser, L.A. Maier, R.P. Baughman, E. Abston, R.C. Bernstein, R. Blankstein, C.A. Bonham, E.S. Chen, D.A. Culver, W. Drake, et al., Diagnosis and detection of sarcoidosis an official American thoracic society clinical practice guideline, Am. J. Respir. Crit. Care Med. 201 (2020) E26–E51.

[77] D.H. Birnie, W.H. Sauer, F. Bogun, J.M. Cooper, D.A. Culver, C.S. Duvernoy, M.A. Judson, J. Kron, D. Mehta, J. Cosedis Nielsen, et al., HRS expert consensus statement on the diagnosis and management of arrhythmias associated with cardiac sarcoidosis, Heart Rhythm 11 (2014) 1304–1323, https://doi.org/10.1016/j.hrthm.2014.03.043.

[78] R.J. Kim, M.R. Patel, P.J. Cawley, J.F. Heitner, I. Klem, M.A. Parker, W.A. Jaroudi, T.J. Meine, J.B. White, M.D. Elliott, et al., Detection of myocardial damage in patients with sarcoidosis, Circulation 120 (2009) 1969–1977, https://doi.org/10.1161/CIRCULATIONAHA.109.851352.

[79] T. Aikawa, N. Oyama-Manabe, M. Naya, H. Ohira, A. Sugimoto, I. Tsujino, M. Obara, O. Manabe, K. Kudo, H. Tsutsui, et al., Delayed contrast-enhanced computed tomography in patients with known or suspected cardiac sarcoidosis: a feasibility study, Eur. Radiol. 27 (10) (2017) 4054–4063.

[80] J. Rubin, M.S. Maurer, Cardiac amyloidosis: overlooked, underappreciated, and treatable, Annu. Rev. Med. 27 (71) (2020) 203–219.

[81] M.D. Benson, J.N. Buxbaum, D.S. Eisenberg, G. Merlini, M.J.M. Saraiva, Y. Sekijima, J.D. Sipe, P. Westermark, Amyloid nomenclature 2018: recommendations by the international society of amyloidosis (ISA) nomenclature committee, Amyloid 25 (2018) 215–219, https://doi.org/10.1080/13506129.2018.1549825.

[82] C.C. Quarta, E. Gonzalez-Lopez, J.A. Gilbertson, N. Botcher, D. Rowczenio, A. Petrie, T. Rezk, T. Youngstein, S. Mahmood, S. Sachchithanantham, et al., Diagnostic sensitivity of abdominal fat aspiration in cardiac amyloidosis, Eur. Heart J. 38 (2017) 1905–1908, https://doi.org/10.1093/eurheartj/ehx047.

[83] G. Treglia, A.W.J.M. Glaudemans, F. Bertagna, B.P.C. Hazenberg, P.A. Erba, R. Giubbini, L. Ceriani, J.O. Prior, L. Giovanella, R.H.J.A. Slart, Diagnostic accuracy of bone scintigraphy in the assessment of cardiac transthyretin-related amyloidosis: a bivariate meta-analysis, Eur. J. Nucl. Med. Mol. Imag. 45 (2018) 1945–1955, https://doi.org/10.1007/s00259-018-4013-4.

[84] S. Bokhari, R. Morgenstern, R. Weinberg, M. Kinkhabwala, D. Panagiotou, A. Castano, A. DeLuca, K. Andrew, Z. Jin, M.S. Maurer, Standardization of 99mTechnetium pyrophosphate imaging methodology to diagnose TTR cardiac amyloidosis, J. Nucl. Cardiol. 25 (2018) 181–190, https://doi.org/10.1007/s12350-016-0610-4.

[85] S. Barros-Gomes, B. Williams, L.F. Nhola, M. Grogan, J.F. Maalouf, A. Dispenzieri, P.A. Pellikka, H.R. Villarraga, Prognosis of light chain amyloidosis with preserved LVEF: added value of 2D speckle-tracking echocardiography to the current prognostic staging system, JACC Cardiovasc Imaging 10 (2017) 398–407, https://doi.org/10.1016/j.jcmg.2016.04.008.

[86] M. Fontana, S.M. Banypersad, T.A. Treibel, A. Abdel-Gadir, V. Maestrini, T. Lane, J.A. Gilbertson, D.F. Hutt, H.J. Lachmann, C.J. Whelan, et al., Differential myocyte responses in patients with cardiac transthyretin amyloidosis and light-chain amyloidosis: a cardiac MR imaging study, Radiology 277 (2015) 388–397, https://doi.org/10.1148/radiol.2015141744.

[87] M. Fontana, S. Pica, P. Reant, A. Abdel-Gadir, T.A. Treibel, S.M. Banypersad, V. Maestrini, W. Barcella, S. Rosmini, H. Bulluck, et al., Prognostic value of late gadolinium enhancement cardiovascular magnetic resonance in cardiac amyloidosis, Circulation 132 (2015) 1570–1579, https://doi.org/10.1161/CIRCULATIONAHA.115.016567.

[88] S. Oda, T. Nakaura, D. Utsunomiya, K. Hirakawa, S. Takashio, Y. Izumiya, K. Tsujita, H. Hata, Y. Ando, Y. Yamashita, Late iodine enhancement and myocardial extracellular volume quantification in cardiac amyloidosis by using dual-energy cardiac computed tomography performed on a dual-layer spectral detector scanner, Amyloid 25 (2018) 137–138.

[89] M. Suzuki, Y. Izawa, T. Toba, A.K. Kono, K. Hirata, Late iodine enhancement and extracellular volume fraction in cardiac amyloidosis by computed tomography, Circ Rep 4 (2022) 145–146, https://doi.org/10.1253/circrep.cr-21-0162.

[90] T. Emoto, S. Oda, M. Kidoh, T. Nakaura, Y. Nagayama, D. Sakabe, K. Kakei, M. Goto, Y. Funama, M. Hatemura, et al., Myocardial extracellular volume quantification using cardiac computed tomography: a comparison of the dual-energy iodine method and the standard subtraction method, Acad. Radiol. 28 (2021) e119–e126, https://doi.org/10.1016/j.acra.2020.03.019.

[91] D. Kassop, M.S. Donovan, M.K. Cheezum, B.T. Nguyen, N.B. Gambill, R. Blankstein, T.C. Villines, Cardiac masses on cardiac CT: a review, Curr Cardiovasc Imaging Rep 7 (2014) 1–13.

[92] M. Gatti, T. D'Angelo, G. Muscogiuri, S. Dell'aversana, A. Andreis, A. Carisio, F. Darvizeh, D. Tore, G. Pontone, R. Faletti, Cardiovascular magnetic resonance of cardiac tumors and masses, World J. Cardiol. 13 (2021) 628–649.

[93] J. Hur, H.N. Pak, Y.J. Kim, H.J. Lee, H.J. Chang, Y.J. Hong, B.W. Choi, Dual-enhancement cardiac computed tomography for assessing left atrial thrombus and pulmonary veins before radiofrequency catheter ablation for atrial fibrillation, Am. J. Cardiol. 112 (2013) 238–244, https://doi.org/10.1016/j.amjcard.2013.03.018.

[94] G. Maccabelli, D. Tsiachris, J. Silberbauer, A. Esposito, C. Bisceglia, F. Baratto, C. Colantoni, N. Trevisi, A. Palmisano, P. Vergara, et al., Imaging and epicardial substrate ablation of ventricular tachycardia in patients late after myocarditis, Europace 16 (2014) 1363–1372, https://doi.org/10.1093/europace/euu017.

[95] T. Dickfeld, J. Tian, G. Ahmad, A. Jimenez, A. Turgeman, R. Kuk, M. Peters, A. Saliaris, M. Saba, S. Shorofsky, et al., MRI-guided ventricular tachycardia ablation integration of late gadolinium-enhanced 3D scar in patients with implantable cardioverter- defibrillators, Circ Arrhythm Electrophysiol 4 (2011) 172–184, https://doi.org/10.1161/CIRCEP.110.958744.

[96] Y. Komatsu, H. Cochet, A. Jadidi, F. Sacher, A. Shah, N. Derval, D. Scherr, P. Pascale, L. Roten, A. Denis, et al., Regional myocardial wall thinning at multidetector computed tomography correlates to arrhythmogenic substrate in postinfarction ventricular tachycardia: assessment of structural and electrical substrate, Circ Arrhythm Electrophysiol 6 (2013) 342–350, https://doi.org/10.1161/CIRCEP.112.000191.

[97] B. Jáuregui, D. Soto-Iglesias, G. Zucchelli, D. Penela, A. Ordóñez, C. Terés, A. Chauca, J. Acosta, J. Fernández-Armenta, M. Linhart, et al., Arrhythmogenic substrate detection in chronic ischaemic patients undergoing ventricular tachycardia ablation using multidetector cardiac computed tomography: compared evaluation with cardiac magnetic resonance, Europace 23 (2021) 82–90, https://doi.org/10.1093/europace/euaa237.

[98] S. Yamashita, F. Sacher, S. Mahida, B. Berte, H.S. Lim, Y. Komatsu, S. Amraoui, A. Denis, N. Derval, F. Laurent, et al., Image integration to guide catheter ablation in scar-related ventricular tachycardia, J. Cardiovasc. Electrophysiol. 27 (2016) 699–708, https://doi.org/10.1111/jce.12963.

[99] E. Conte, C. Carbucicchio, V. Catto, A.N. Kochi, S. Mushtaq, P.G. De Iuliis, M. Guglielmo, A. Baggiano, T. Sattin, G. Pontone, et al., Live integration of comprehensive cardiac CT with electroanatomical mapping in patients with refractory ventricular tachycardia, J Cardiovasc Comput Tomogr 16 (2022) 262–265, https://doi.org/10.1016/j.jcct.2021.12.003.

[100] E. Conte, S. Mushtaq, C. Carbucicchio, G. Piperno, V. Catto, M.E. Mancini, A. Formenti, A. Annoni, M. Guglielmo, A. Baggiano, et al., State of the art paper: cardiovascular CT for planning ventricular tachycardia ablation procedures, J Cardiovasc Comput Tomogr 15 (2021) 394–402.

[101] R. Mehran, G.D. Dangas, S.D. Weisbord, Contrast-associated acute kidney injury, N. Engl. J. Med. 380 (2019) 2146–2155, https://doi.org/10.1056/nejmra1805256.

[102] American College of Radiology. Committee on Drugs and Contrast Media *ACR Manual On Contrast Media*; ISBN 9781559030120.

[103] J. Shao, J.S. Jiang, X.Y. Wang, S.M. Wu, J. Xiao, K.L. Zheng, R.X. Qi, Measurement of myocardial extracellular volume using cardiac dual-energy computed tomography in patients with ischaemic cardiomyopathy: a comparison of different methods, Int. J. Cardiovasc. Imag. 38 (2022) 1591–1600, https://doi.org/10.1007/s10554-022-02532-z.
[104] M.J. Willemink, M. Persson, A. Pourmorteza, N.J. Pelc, D. Fleischmann, Photon-counting CT: technical principles and clinical prospects, Radiology 289 (2018) 293–312.
[105] A. Sabarudin, T.W. Siong, A.W. Chin, N.K. Hoong, M.K.A. Karim, A comparison study of radiation effective dose in ECG-gated coronary CT angiography and calcium scoring examinations performed with a dual-source CT scanner, Sci. Rep. 9 (2019), https://doi.org/10.1038/s41598-019-40758-5.
[106] R. Symons, V. Sandfort, M. Mallek, S. Ulzheimer, A. Pourmorteza, Coronary artery calcium scoring with photon-counting CT: first in vivo human experience, Int. J. Cardiovasc. Imag. 35 (2019) 733–739, https://doi.org/10.1007/s10554-018-1499-6.
[107] S. Kappler, T. Hannemann, E. Kraft, B. Kreisler, D. Niederloehner, K. Stierstorfer, T. Flohr, First results from a hybrid prototype CT scanner for exploring benefits of quantum-counting in clinical CT, in: Proceedings of the Medical Imaging 2012: Physics of Medical Imaging vol. 8313, February 23 2012, p. 83130X. SPIE.
[108] A. Pourmorteza, R. Symons, D.S. Reich, M. Bagheri, T.E. Cork, S. Kappler, S. Ulzheimer, D.A. Bluemke, Photon-counting CT of the brain: in vivo human results and image-quality assessment, Am. J. Neuroradiol. 38 (2017) 2257–2263, https://doi.org/10.3174/ajnr.A5402.
[109] R. Gutjahr, A.F. Halaweish, Z. Yu, S. Leng, L. Yu, Z. Li, S.M. Jorgensen, E.L. Ritman, S. Kappler, C.H. McCollough, Human imaging with photon counting-based computed tomography at clinical dose levels: contrast-to-noise ratio and cadaver studies, Invest. Radiol. 51 (2016) 421–429, https://doi.org/10.1097/RLI.0000000000000251.
[110] R. Symons, Y. De Bruecker, J. Roosen, L. Van Camp, T.E. Cork, S. Kappler, S. Ulzheimer, V. Sandfort, D.A. Bluemke, A. Pourmorteza, Quarter-millimeter spectral coronary stent imaging with photon-counting CT: initial experience, J Cardiovasc Comput Tomogr 12 (2018) 509–515, https://doi.org/10.1016/j.jcct.2018.10.008.
[111] M. Mannil, T. Hickethier, J. Von Spiczak, M. Baer, A. Henning, M. Hertel, B. Schmidt, T. Flohr, D. Maintz, H. Alkadhi, Photon-counting CT: high-resolution imaging of coronary stents, Invest. Radiol. 53 (2018) 143–149, https://doi.org/10.1097/RLI.0000000000000420.
[112] G. Cundari, P. Deilmann, V. Mergen, K. Ciric, M. Eberhard, L. Jungblut, H. Alkadhi, K. Higashigaito, Saving contrast media in coronary CT angiography with photon-counting detector CT, Acad. Radiol. 31 (2024) 212–220, https://doi.org/10.1016/j.acra.2023.06.025.
[113] N. Oyama-Manabe, S. Oda, Y. Ohta, H. Takagi, K. Kitagawa, M. Jinzaki, Myocardial late enhancement and extracellular volume with single-energy, dual-energy, and photon-counting computed tomography, J Cardiovasc Comput Tomogr 18 (2024) 3–10.
[114] D.P. Cormode, E. Roessl, A. Thran, T. Skajaa, R.E. Gordon, J.-P. Schlomka, V. Fuster, E.A. Fisher, W.J.M. Mulder, R. Proksa, et al., Atherosclerotic Plaque Composition: Analysis with Multicolor CT and Targeted Gold Nanoparticles 1 256 (2010), https://doi.org/10.1148/radiol.10092473/-/DC1.
[115] R. Symons, T.E. Cork, M.N. Lakshmanan, R. Evers, C. Davies-Venn, K.A. Rice, M.L. Thomas, C.Y. Liu, S. Kappler, S. Ulzheimer, et al., Dual-contrast agent photon-counting computed tomography of the heart: initial experience, Int. J. Cardiovasc. Imag. 33 (2017) 1253–1261, https://doi.org/10.1007/s10554-017-1104-4.
[116] H. Bornefalk, M. Danielsson, Photon-counting spectral computed tomography using silicon strip detectors: a feasibility study, Phys. Med. Biol. 55 (2010) 1999–2022, https://doi.org/10.1088/0031-9155/55/7/014.
[117] M. Touch, D.P. Clark, W. Barber, C.T. Badea, A neural network-based method for spectral distortion correction in photon counting x-ray CT, Phys. Med. Biol. 61 (2016) 6132–6153, https://doi.org/10.1088/0031-9155/61/16/6132.
[118] B.V. Becker, H.L. Kaatsch, K. Nestler, D. Overhoff, J. Schneider, D. Dillinger, J. Piechotka, M.A. Brockmann, R. Ullmann, M. Port, et al., Initial experience on abdominal photon-counting computed tomography in clinical routine: general image quality and dose exposure, Eur. Radiol. (2022), https://doi.org/10.1007/s00330-022-09278-1.
[119] F. Risch, F. Schwarz, F. Braun, S. Bette, J. Becker, C. Scheurig-Muenkler, T.J. Kroencke, J.A. Decker, Assessment of epicardial adipose tissue on virtual non-contrast images derived from photon-counting detector coronary CTA datasets, Eur. Radiol. (2022), https://doi.org/10.1007/s00330-022-09257-6.
[120] A. Meloni, E. Maffei, A. Clemente, C. De Gori, M. Occhipinti, V. Positano, S. Berti, L. La Grutta, L. Saba, R. Cau, et al., Spectral photon-counting computed tomography: technical principles and applications in the assessment of cardiovascular diseases, J. Clin. Med. 13 (2024) 2359, https://doi.org/10.3390/jcm13082359.
[121] F. Cademartiri, A. Meloni, L. Pistoia, G. Degiorgi, A. Clemente, C. De Gori, V. Positano, S. Celi, S. Berti, M. Emdin, et al., Dual-source photon-counting computed tomography—Part I: clinical overview of cardiac CT and coronary CT angiography applications, J. Clin. Med. 12 (2023).
[122] C. Zanon, F. Cademartiri, A. Toniolo, C. Bini, A. Clemente, E.C. Colacchio, G. Cabrelle, F. Mastro, M. Antonello, E. Quaia, et al., Advantages of photon-counting detector CT in aortic imaging, Tomography 10 (2024) 1–13.